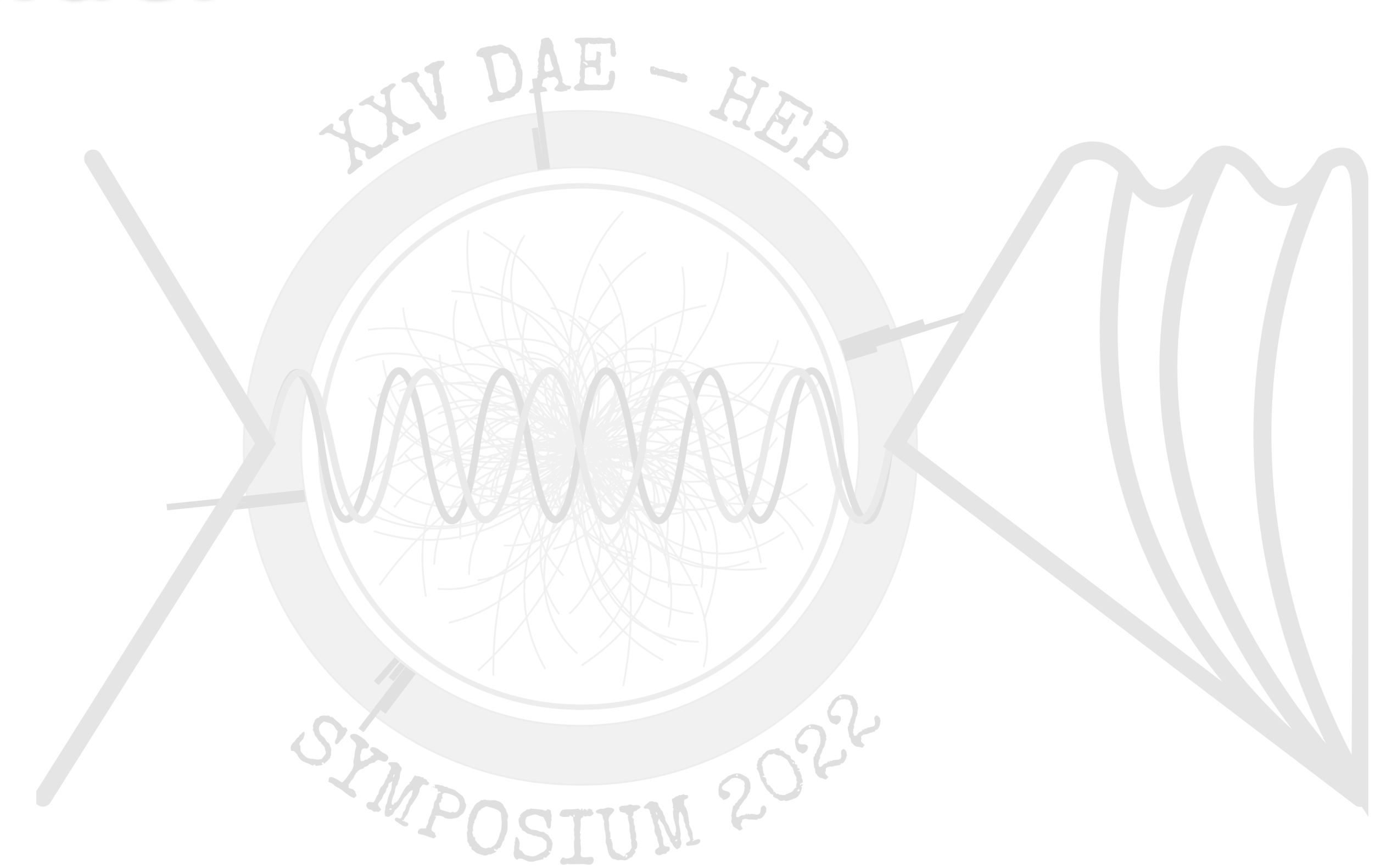


Probing Anomalous Couplings in Single Higgs Production at ep Collider

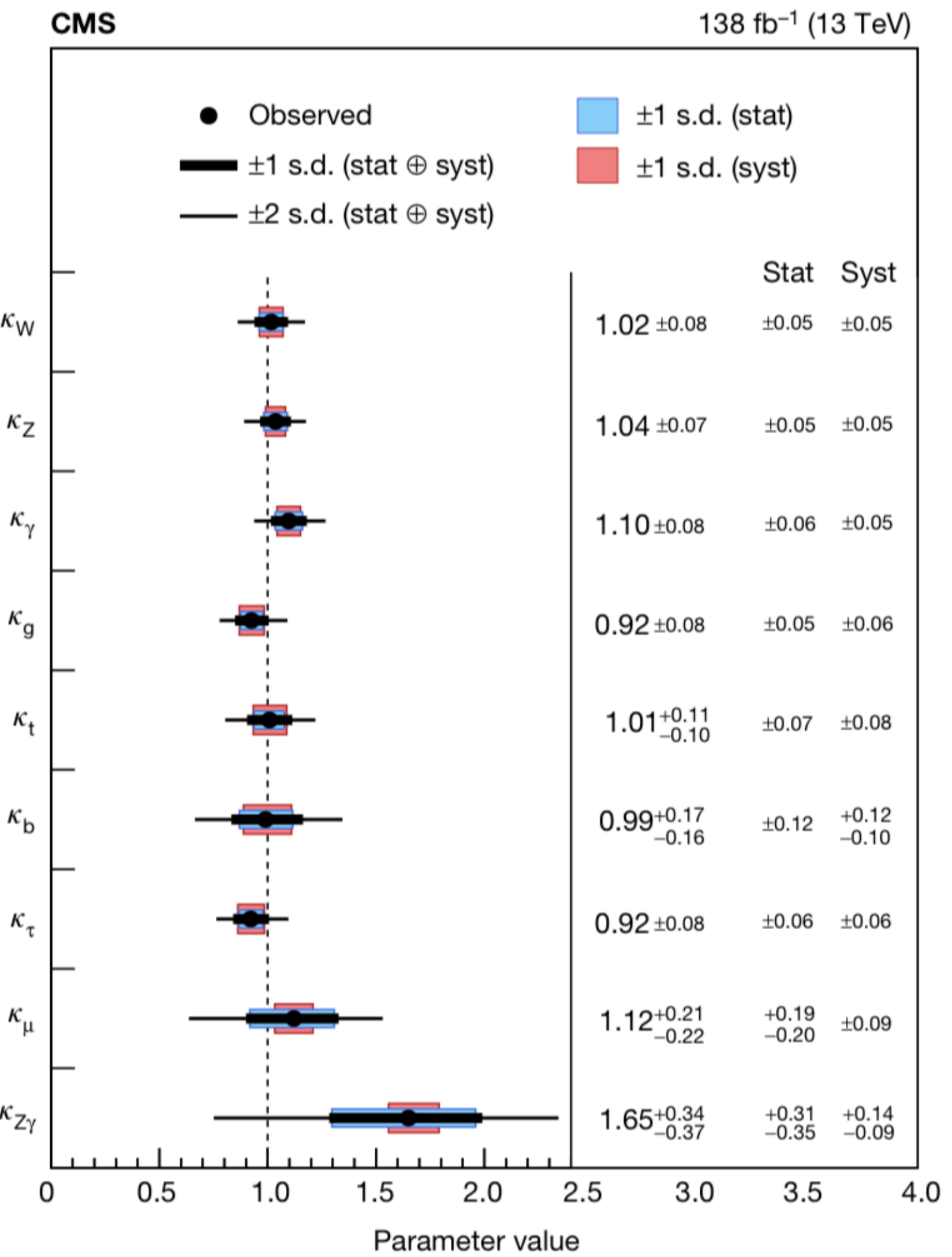
Pramod Sharma and Ambresh Shivaji, JHEP 10 (2022) 108

Pramod Sharma
IISER Mohali, India



XXV DAE-BRNS High Energy Physics
Symposium 2022
Dec 12-16, 2022

- A particle of 125 GeV discovered by CMS and ATLAS experiments in 2012
- So far measurements of Higgs boson properties are compatible with SM within current uncertainties
- The **KEY** to probe new physics is to verify EWSB (Higgs mechanism)
- Uncertainty $\rightarrow \approx 10\%$ in Higgs to gauge boson couplings



Ref. [1] Nature 607, 60-68 (2022)

Anomalous $HVV(V = W^\pm, Z)$ coupling

Most general Lagrangian

$$g \left(m_W \kappa_W W_\mu^+ W^{-\mu} + \frac{\kappa_Z}{2 \cos \theta_W} m_Z Z_\mu Z^\mu \right) H$$

$g \rightarrow SU(2)$ coupling parameter

$$\begin{aligned} & -\frac{g}{m_W} \left[\frac{\lambda_{1W}}{2} W^{+\mu\nu} W^-_{\mu\nu} + \frac{\lambda_{1Z}}{4} Z^{\mu\nu} Z_{\mu\nu} \right. \\ & \left. + \lambda_{2W} (W^{+\nu} \partial^\mu W^-_{\mu\nu} + h.c.) + \lambda_{2Z} Z^\nu \partial^\mu Z_{\mu\nu} \right] \end{aligned}$$

$$+ \frac{\tilde{\lambda}_W}{2} W^{+\mu\nu} \widetilde{W}^-_{\mu\nu} + \frac{\tilde{\lambda}_Z}{4} Z^{\mu\nu} \widetilde{Z}_{\mu\nu} \Big] H$$

$$\tilde{V}^{\mu\nu} = \frac{1}{2} \epsilon^{\mu\nu\alpha\beta} V_{\alpha\beta}$$

$$V^{\mu\nu} = \partial^\mu V^\nu - \partial^\nu V^\mu$$

Anomalous $HVV(V = W^\pm, Z)$ coupling

Most general Lagrangian

$$\left. \begin{aligned} & g \left(m_W \kappa_W W_\mu^+ W^{-\mu} + \frac{\kappa_Z}{2 \cos \theta_W} m_Z Z_\mu Z^\mu \right) H \\ & - \frac{g}{m_W} \left[\frac{\lambda_{1W}}{2} W^{+\mu\nu} W^-_{\mu\nu} + \frac{\lambda_{1Z}}{4} Z^{\mu\nu} Z_{\mu\nu} \right. \\ & + \lambda_{2W} (W^{+\nu} \partial^\mu W^-_{\mu\nu} + h.c.) + \lambda_{2Z} Z^\nu \partial^\mu Z_{\mu\nu} \\ & \left. + \frac{\tilde{\lambda}_W}{2} W^{+\mu\nu} \widetilde{W}^-_{\mu\nu} + \frac{\tilde{\lambda}_Z}{4} Z^{\mu\nu} \widetilde{Z}_{\mu\nu} \right] H \end{aligned} \right\}$$

SM like

Derivative of fields

Anomalous $HVV(V = W^\pm, Z)$ coupling

Most general Lagrangian

$$\begin{aligned} & g \left(m_W \kappa_W W_\mu^+ W^{-\mu} + \frac{\kappa_Z}{2 \cos \theta_W} m_Z Z_\mu Z^\mu \right) H \\ & - \frac{g}{m_W} \left[\frac{\lambda_{1W}}{2} W^{+\mu\nu} W^-_{\mu\nu} + \frac{\lambda_{1Z}}{4} Z^{\mu\nu} Z_{\mu\nu} \right. \\ & + \lambda_{2W} (W^{+\nu} \partial^\mu W^-_{\mu\nu} + h.c.) + \lambda_{2Z} Z^\nu \partial^\mu Z_{\mu\nu} \\ & \left. + \frac{\tilde{\lambda}_W}{2} W^{+\mu\nu} \widetilde{W}^-_{\mu\nu} + \frac{\tilde{\lambda}_Z}{4} Z^{\mu\nu} \widetilde{Z}_{\mu\nu} \right] H \end{aligned}$$

SM like

CP even

Derivative of fields

CP odd

Anomalous $HVV(V = W^\pm, Z)$ coupling

Most general Lagrangian

$$g \left(m_W \kappa_W W_\mu^+ W^{-\mu} + \frac{\kappa_Z}{2 \cos \theta_W} m_Z Z_\mu Z^\mu \right) H$$

$$-\frac{g}{m_W} \left[\frac{\lambda_{1W}}{2} W^{+\mu\nu} W^-_{\mu\nu} + \frac{\lambda_{1Z}}{4} Z^{\mu\nu} Z_{\mu\nu} \right]$$

$$+ \lambda_{2W} (W^{+\nu} \partial^\mu W^-_{\mu\nu} + h.c.) + \lambda_{2Z} Z^\nu \partial^\mu Z_{\mu\nu}$$

$$+ \frac{\tilde{\lambda}_W}{2} W^{+\mu\nu} \widetilde{W}^-_{\mu\nu} + \frac{\tilde{\lambda}_Z}{4} Z^{\mu\nu} \widetilde{Z}_{\mu\nu} \right] H$$

Vertex form

$$\Gamma_{HVV}^{\mu\nu}(p_1, p_2)$$

$$g_V m_V \kappa_V g^{\mu\nu}$$

$$+ \frac{g}{m_W} \left[\lambda_{1V} (p_1^\nu p_2^\mu - g^{\mu\nu} p_1 \cdot p_2) \right.$$

$$+ \lambda_{2V} (p_1^\mu p_1^\nu + p_2^\mu p_2^\nu - g^{\mu\nu} p_1 \cdot p_1 - g^{\mu\nu} p_2 \cdot p_2)$$

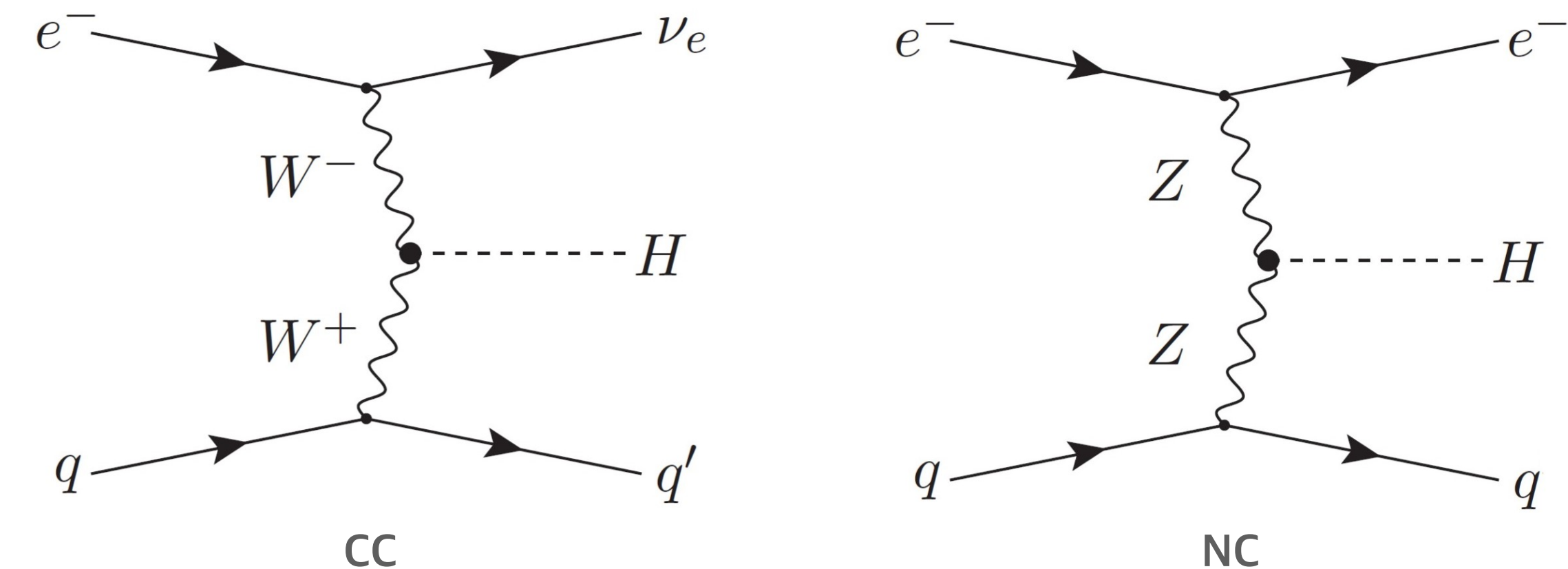
$$+ \tilde{\lambda}_V \epsilon^{\mu\nu\alpha\beta} p_{1\alpha} p_{2\beta} \left. \right]$$

ep Collider

Collider	Center of mass energy (TeV)	Process	Cross section (pb)
pp	14	$pp \rightarrow hjj$	3.7
ILC	1	$e^+e^- \rightarrow e^+e^-h$	0.007
		$e^+e^- \rightarrow \nu_e \bar{\nu}_e h$	0.21
CLIC	3	$e^+e^- \rightarrow e^+e^-h$	6×10^{-4}
		$e^+e^- \rightarrow \nu_e \bar{\nu}_e h$	0.5
LHeC	1.3	$e^-p \rightarrow e^-hj$	0.016
		$e^-p \rightarrow \nu_e hj$	0.088

For this study, $E_e = 60$ GeV, $E_p = 7$ TeV

- **LHeC:** e^- energy 60 to 120 GeV with 7 TeV proton energy
- Sufficiently large cross section as compared to e^+e^- collider
- Clean environment with suppressed background as compared to pp collider



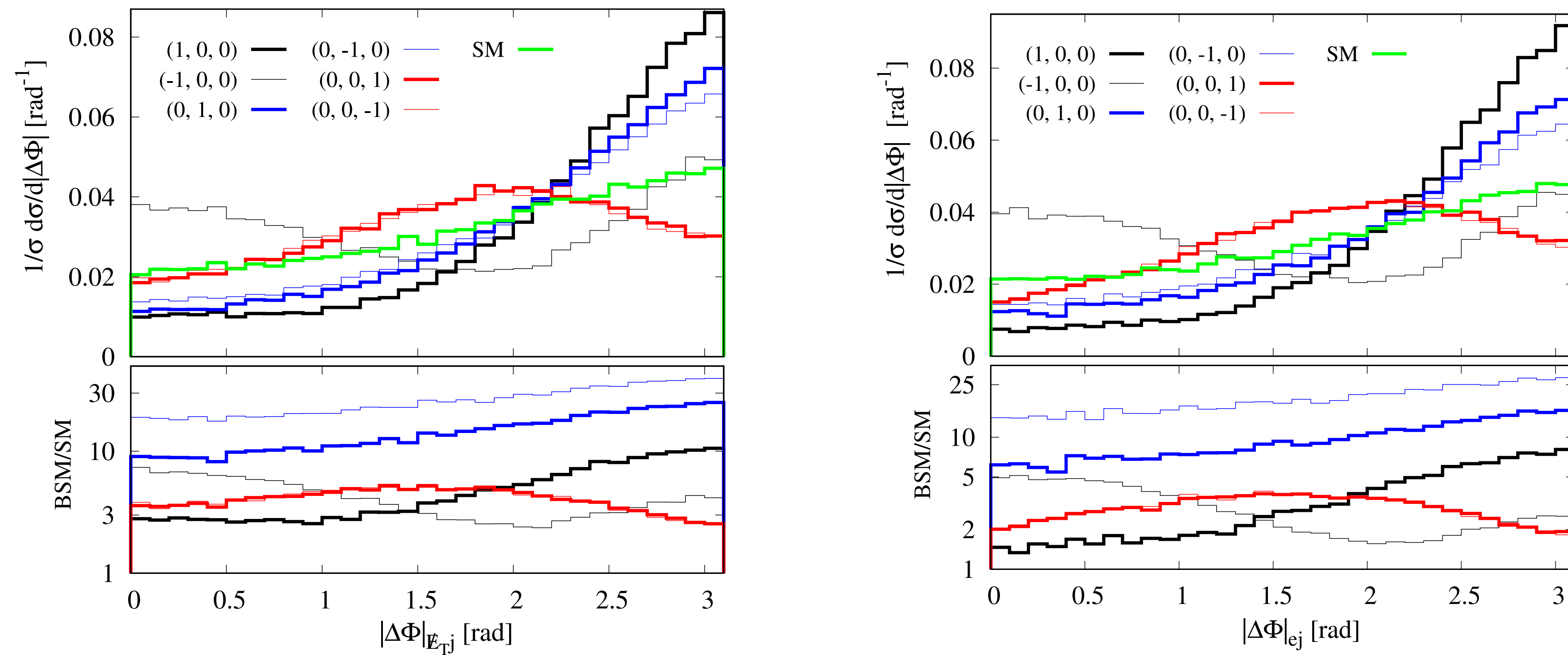
Results and discussion

Observables: $|\Delta\phi|$ is azimuthal correlation of two particles 1 and 2

$$|\Delta\phi| = \cos^{-1}(\hat{p}_{T1} \cdot \hat{p}_{T2})$$

Motivation: $|\Delta\phi|$ distribution is a good observable to distinguish CP-even and CP-odd couplings of CC process considered in ref. [2]

Results



BSM effects in $|\Delta\phi|$ distribution for CC (left) and NC (right)
 $(\lambda_{1V}, \lambda_{2V}, \tilde{\lambda}_V)$

- $|\Delta\phi|$ is sensitive to individual effect of new couplings
- Deviation in distribution with respect to SM is largest for λ_{2V} and smallest for $\tilde{\lambda}_V$

Results

Signal for CC (NC) $e^- p \rightarrow \nu_e(e^-)hj, h \rightarrow b\bar{b}$ $j = g, u, d, s, c$

Results

Signal for CC (NC) $e^- p \rightarrow \nu_e(e^-)hj, h \rightarrow b\bar{b}$ $j = g, u, d, s, c$

Background for CC (NC)

- Irreducible background : $e^- p \rightarrow \nu_e(e^-)b\bar{b}j$

Results

Signal for CC (NC) $e^- p \rightarrow \nu_e(e^-)hj, h \rightarrow b\bar{b}$ $j = g, u, d, s, c$

Background for CC (NC)

- Irreducible background : $e^- p \rightarrow \nu_e(e^-)b\bar{b}j$
- Reducible background: $\left\{ \begin{array}{l} e^- p \rightarrow \nu_e(e^-)jjj \\ e^- p \rightarrow \nu_e(e^-)bbjj \end{array} \right.$

Photo production from $e^- p \rightarrow e^- b\bar{b}j$



$$\gamma^* p \rightarrow b\bar{b}j \text{ for CC process}$$

Results

Signal for CC (NC) $e^- p \rightarrow \nu_e(e^-)hj, h \rightarrow b\bar{b}$ $j = g, u, d, s, c$

Background for CC (NC)

- Irreducible background : $e^- p \rightarrow \nu_e(e^-)b\bar{b}j$

Negligible for miss-tagging rates

c jet $\rightarrow 0.1$

light jet $\rightarrow 0.01$

- Reducible background:

Reduced by E_T for a very collinear
 e^- along the beam pipe

$e^- p \rightarrow \nu_e(e^-)jjj$

$e^- p \rightarrow \nu_e(e^-)bbjj$

Photo production from $e^- p \rightarrow e^- b\bar{b}j$



$\gamma^* p \rightarrow b\bar{b}j$ for CC process

Results

Signal for CC (NC) $e^- p \rightarrow \nu_e(e^-)hj, h \rightarrow b\bar{b}$ $j = g, u, d, s, c$

Background for CC (NC)

- Irreducible background : $e^- p \rightarrow \nu_e(e^-)b\bar{b}j$ ✓
 - Reducible background:
 - $e^- p \rightarrow \nu_e(e^-)jjj$
 - $e^- p \rightarrow \nu_e(e^-)bbjj$ ✓
- Reduced by E_T for a very collinear e^- along the beam pipe
- Negligible for miss-tagging rates
 c jet $\rightarrow 0.1$
light jet $\rightarrow 0.01$
- Photo production from $e^- p \rightarrow e^- b\bar{b}j$
- $\gamma^* p \rightarrow b\bar{b}j$ for CC process

Results

Signal for CC (NC) $e^- p \rightarrow \nu_e(e^-)hj, h \rightarrow b\bar{b}$ $j = g, u, d, s, c$

Background for CC (NC)

- Irreducible background : $e^- p \rightarrow \nu_e(e^-)b\bar{b}j$ ✓
- Reducible background: { $e^- p \rightarrow \nu_e(e^-)jjj$ (gray box)
 $e^- p \rightarrow \nu_e(e^-)bbjj$ ✓

Negligible for miss-tagging rates
c jet → 0.1
light jet → 0.01

Energy smearing of partons by $\frac{\sigma_E}{E} = a/\sqrt{E} \oplus b$

a = 0.6, b= 0.04 for jets, a= 0.12, b=0.02 for electrons [3]

Results

Signal v/s background

Cuts or CC

$p_T(j) > 30 \text{ GeV}, p_T(b) > 30 \text{ GeV}, E_T > 25 \text{ GeV}$

$|M_{b\bar{b}} - m_H| < 15 \text{ GeV}$

$1 < \eta_j < 5.0, -1 < \eta_b < 4.0, M_{Hj} > 250 \text{ GeV}$

Cuts or NC

$p_T(e) > 20 \text{ GeV}, p_T(j) > 30 \text{ GeV}, p_T(b) > 30 \text{ GeV}$

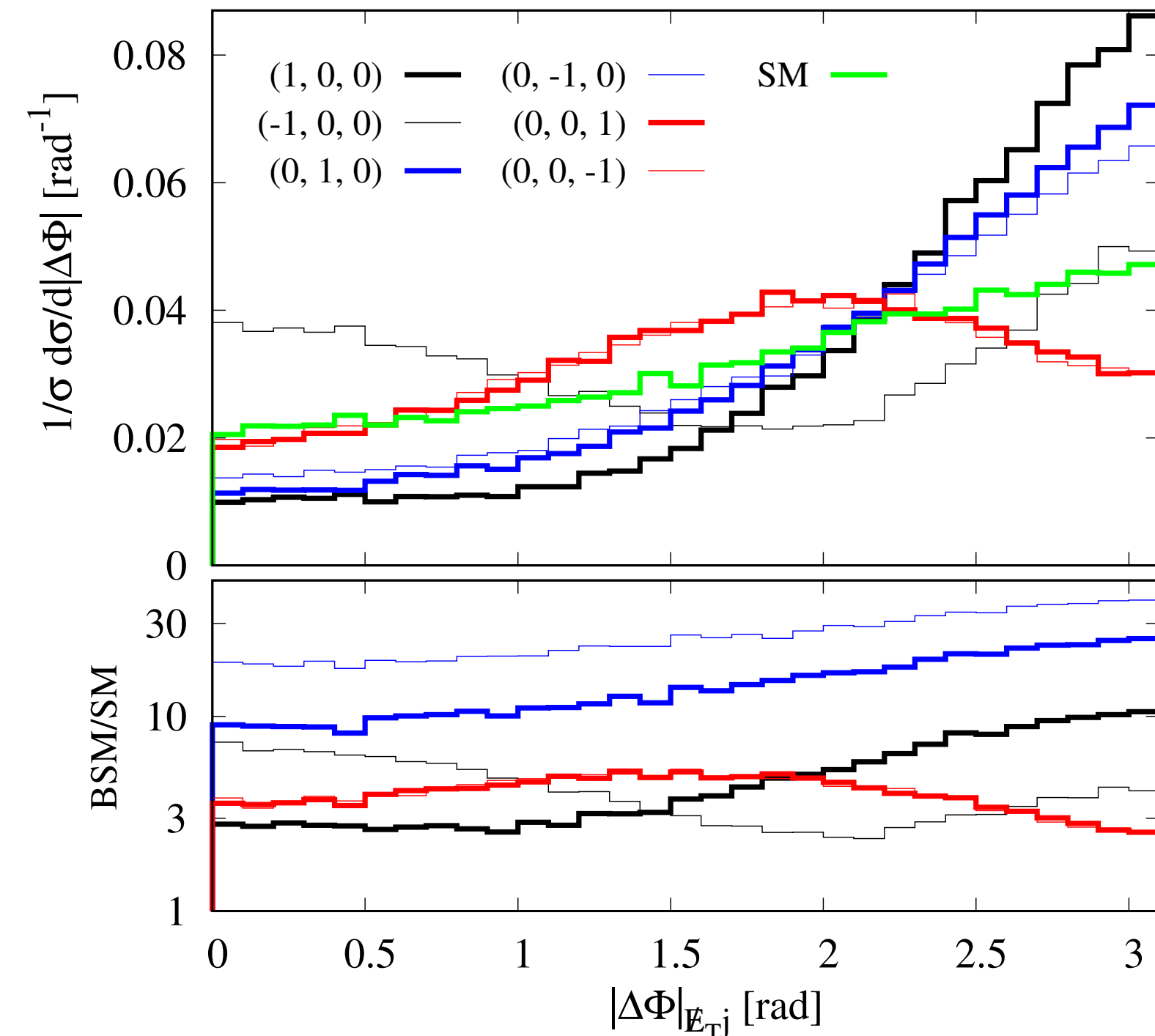
$|M_{b\bar{b}} - m_H| < 15 \text{ GeV}$

$|\eta_e| < 2.5, 2 < \eta_j < 5.0, 0.5 < \eta_b < 4.0, M_{Hj} > 300 \text{ GeV}$

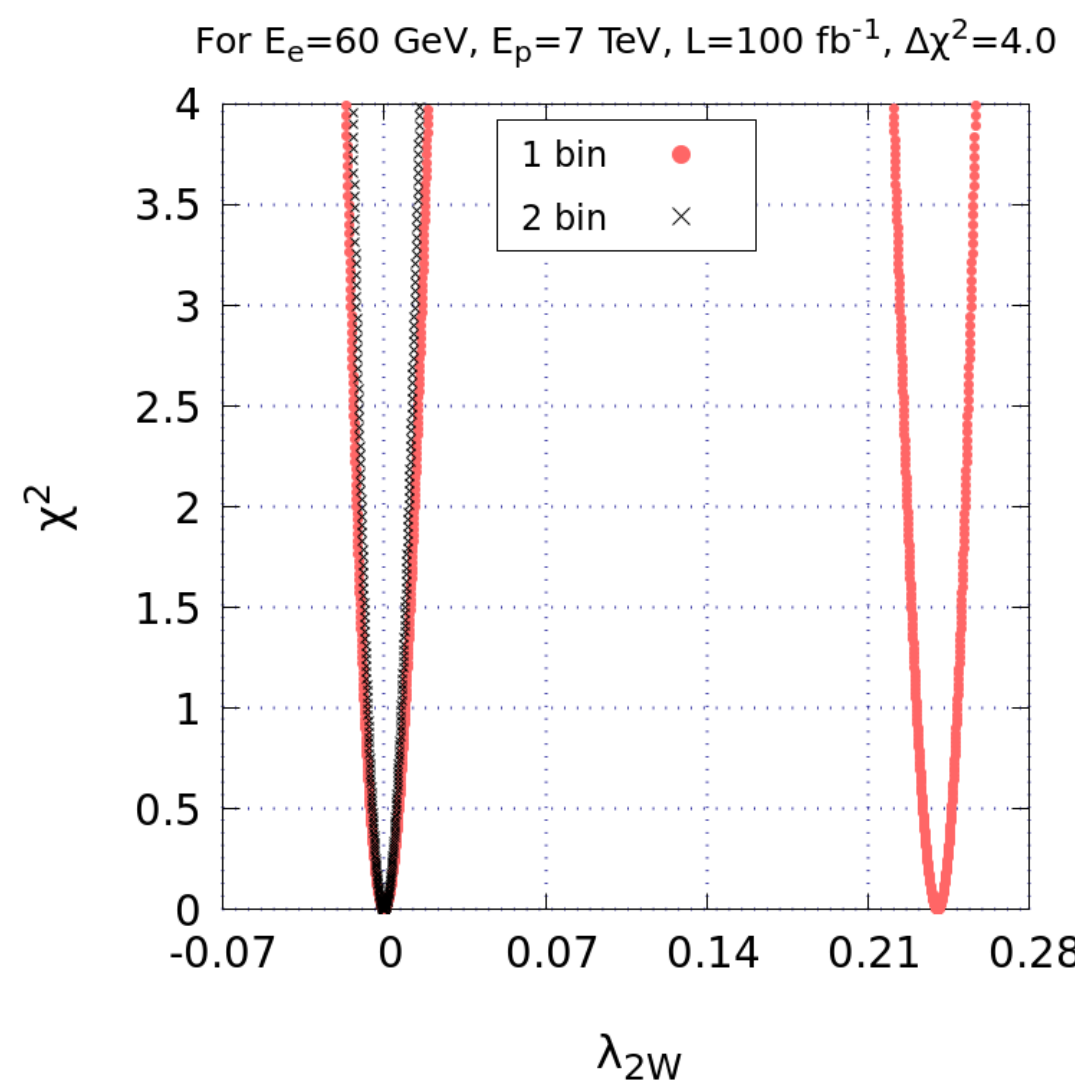
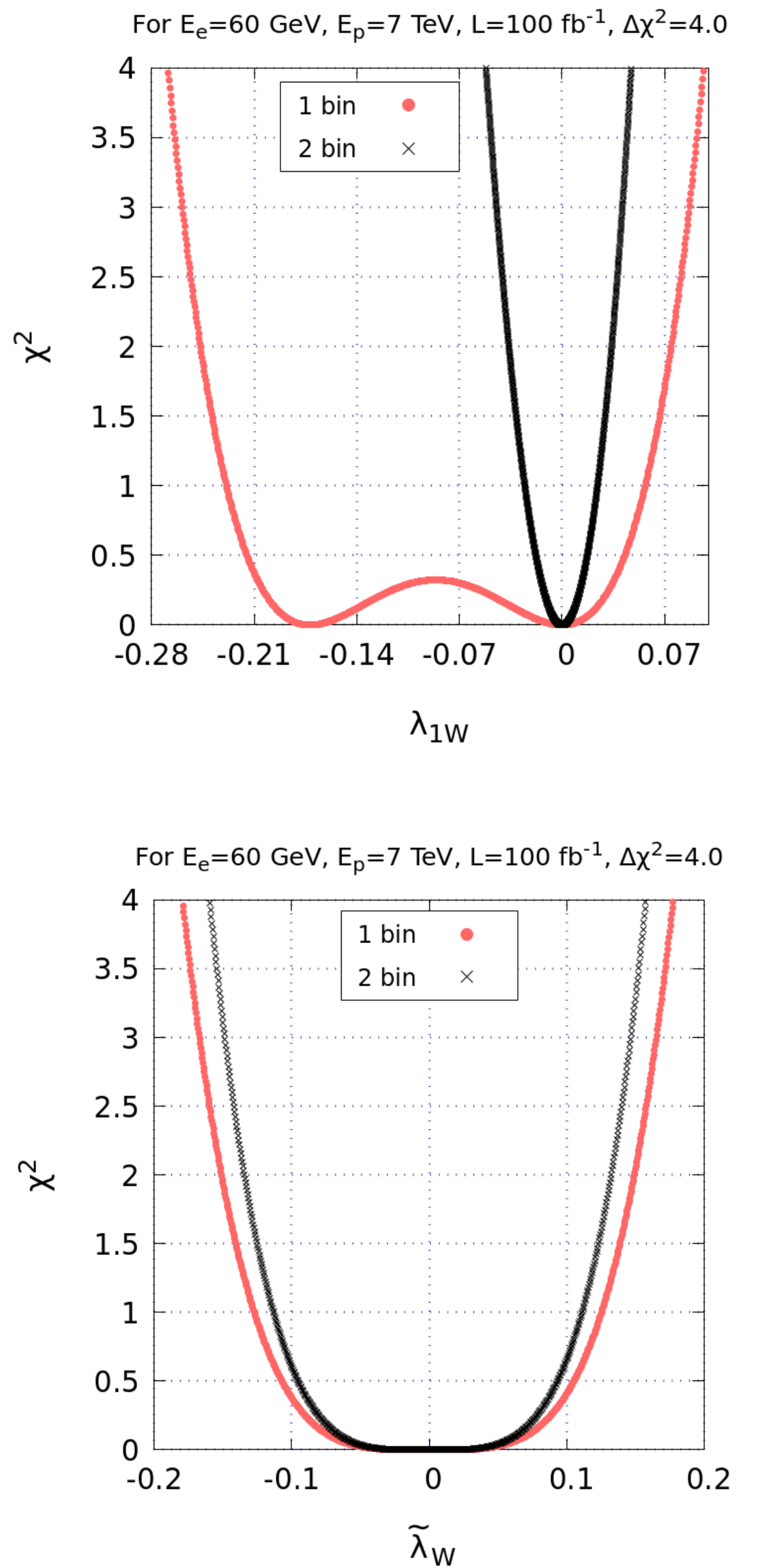
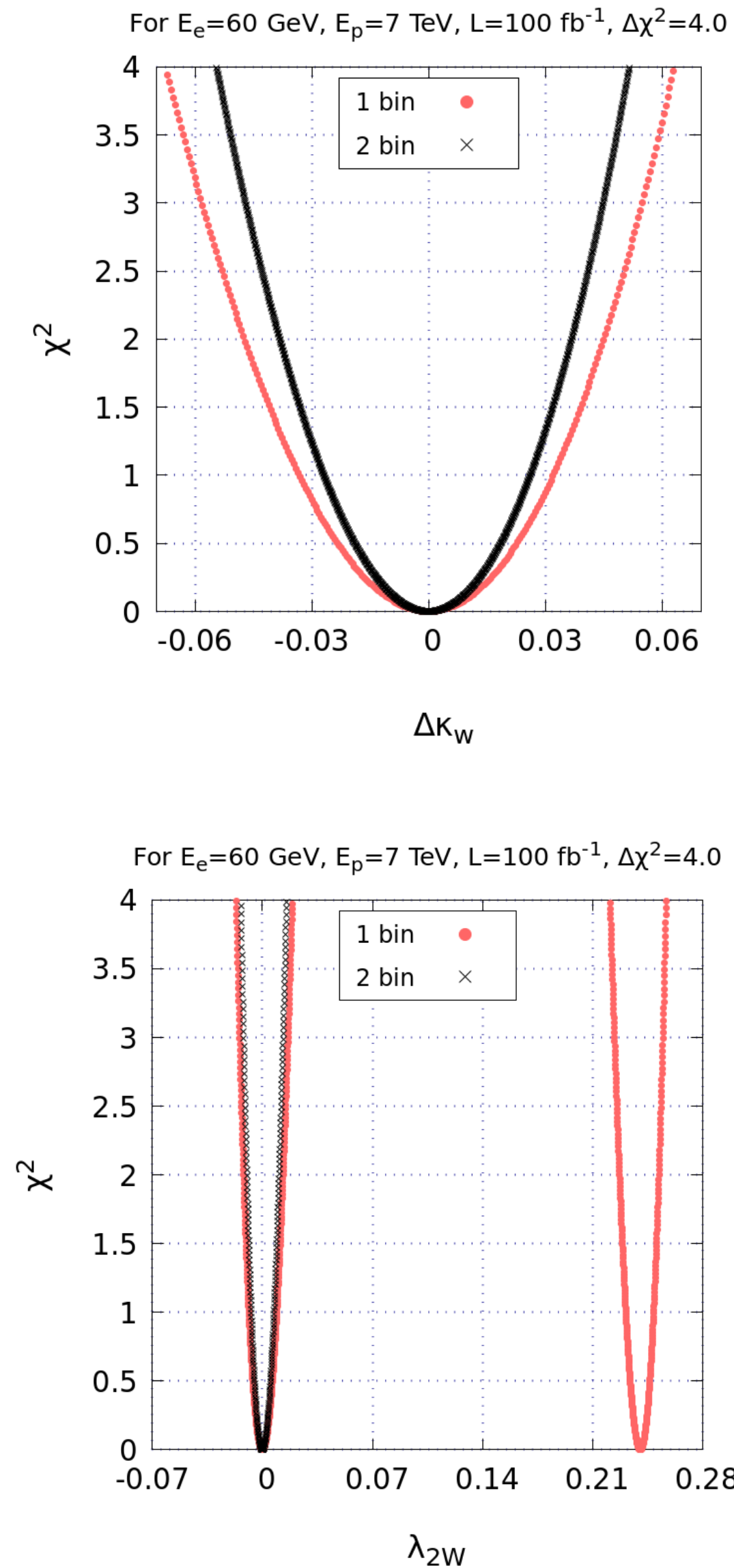
Process	Events at generation level	Events after cuts
Signal	3011	819
$\nu_e b\bar{b}j$	18883	30
$\nu_e b\bar{b}jj$	10985	38
S/B	0.1	12.0

Process	Events at generation level	Events after cuts
Signal	534	76
$e^- b\bar{b}j$	2.75×10^6	161
$e^- b\bar{b}jj$	6.3×10^5	24
S/B	0.02×10^{-2}	0.41

Constraints on HWW parameters at $L = 100 \text{ fb}^{-1}$



- λ_{2W} is constrained most while $\tilde{\lambda}_W$ is constrained least
- Very small effect of 2 bin analysis on κ_W and $\tilde{\lambda}_W$



$\tilde{\lambda}_W$

λ_{2W}

λ_{1W}

Constraints on HWW parameters at $L = 100 \text{ fb}^{-1}$

at 95% C.L.

	Our limits at $L = 100 \text{ fb}^{-1}$	Run II data [a] $35.9 \text{ fb}^{-1}, 13 \text{ TeV}$	HL LHC [e] 3.4%
$\kappa_W \rightarrow$	[0.94, 1.05]		
$\tilde{\lambda}_W \rightarrow$	[-0.16, 0.16]	Run II LHC [b]	FCC eh [d] $1 \text{ ab}^{-1}, 3.5 \text{ TeV}$
$\lambda_{1W} \rightarrow$	[-0.05, 0.05]		LHeC [c] $0.5 \text{ ab}^{-1}, E_e = 140 \text{ GeV}, E_p = 6.5 \text{ GeV}$
$\lambda_{2W} \rightarrow$	[-0.013, 0.015]	FCC eh [d] $[-0.05, 0.05]$	[-0.06, 0.1]

[a] Eur. Phys. J. C 79 (2019) 421 [arXiv:1809.10733]

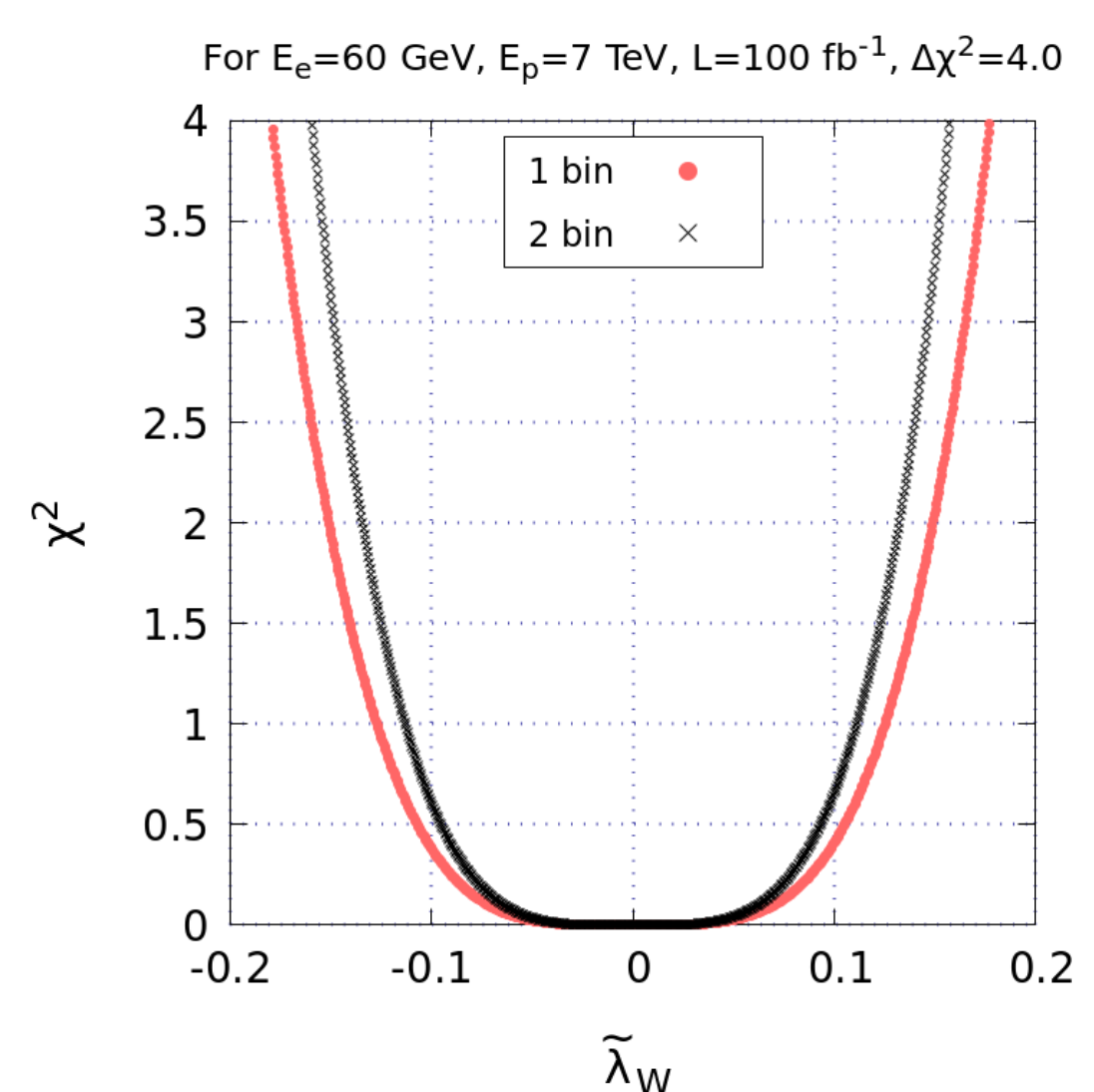
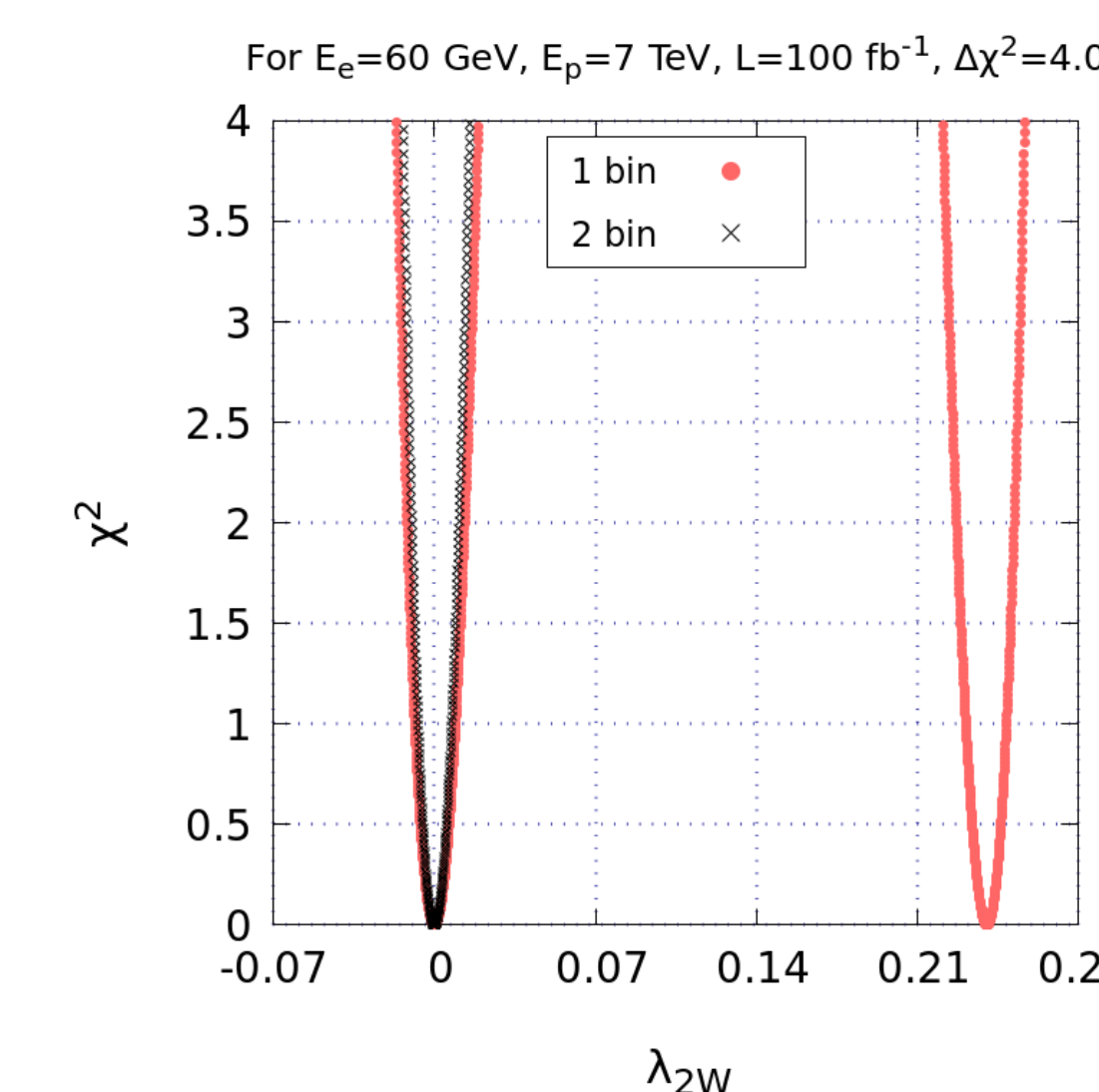
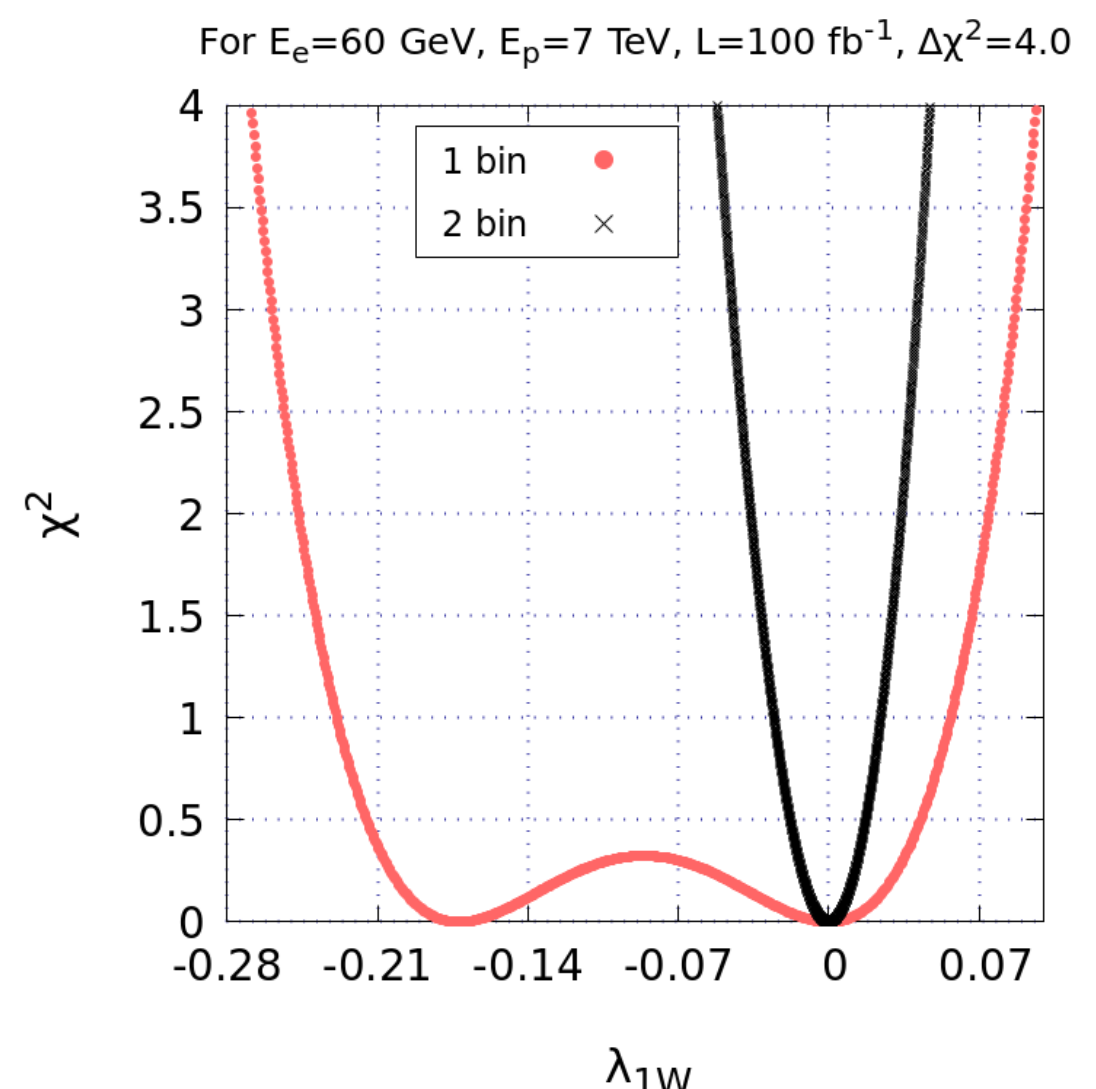
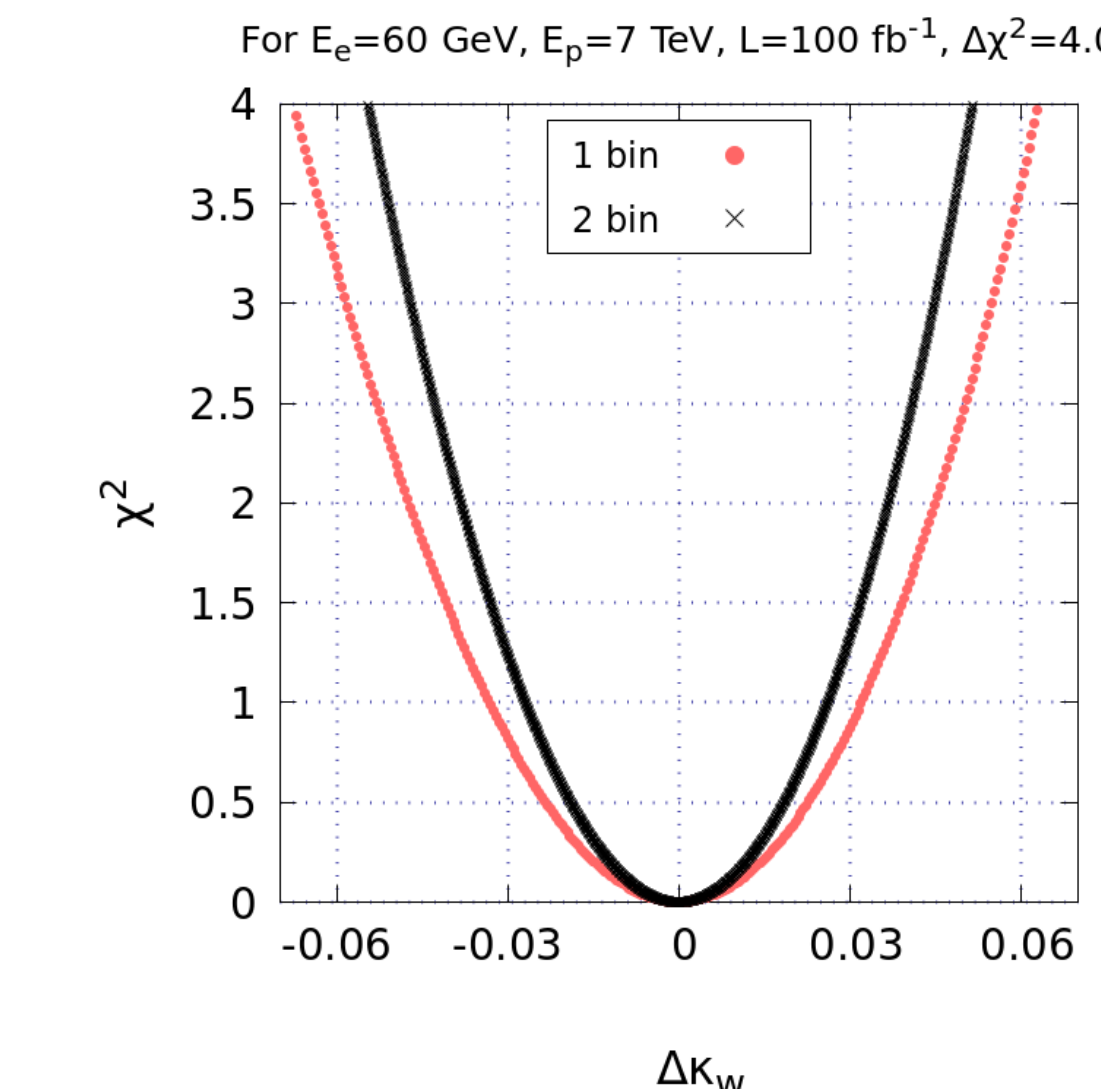
[b] Phys. Lett. B 805 (2020) 135426 [arXiv:2002.05315]

[c] arXiv:1203.6285

[d] arXiv:1509.04016

[e] arXiv:1902.00134

Constraints on HWW parameters at $L = 100 \text{ fb}^{-1}$



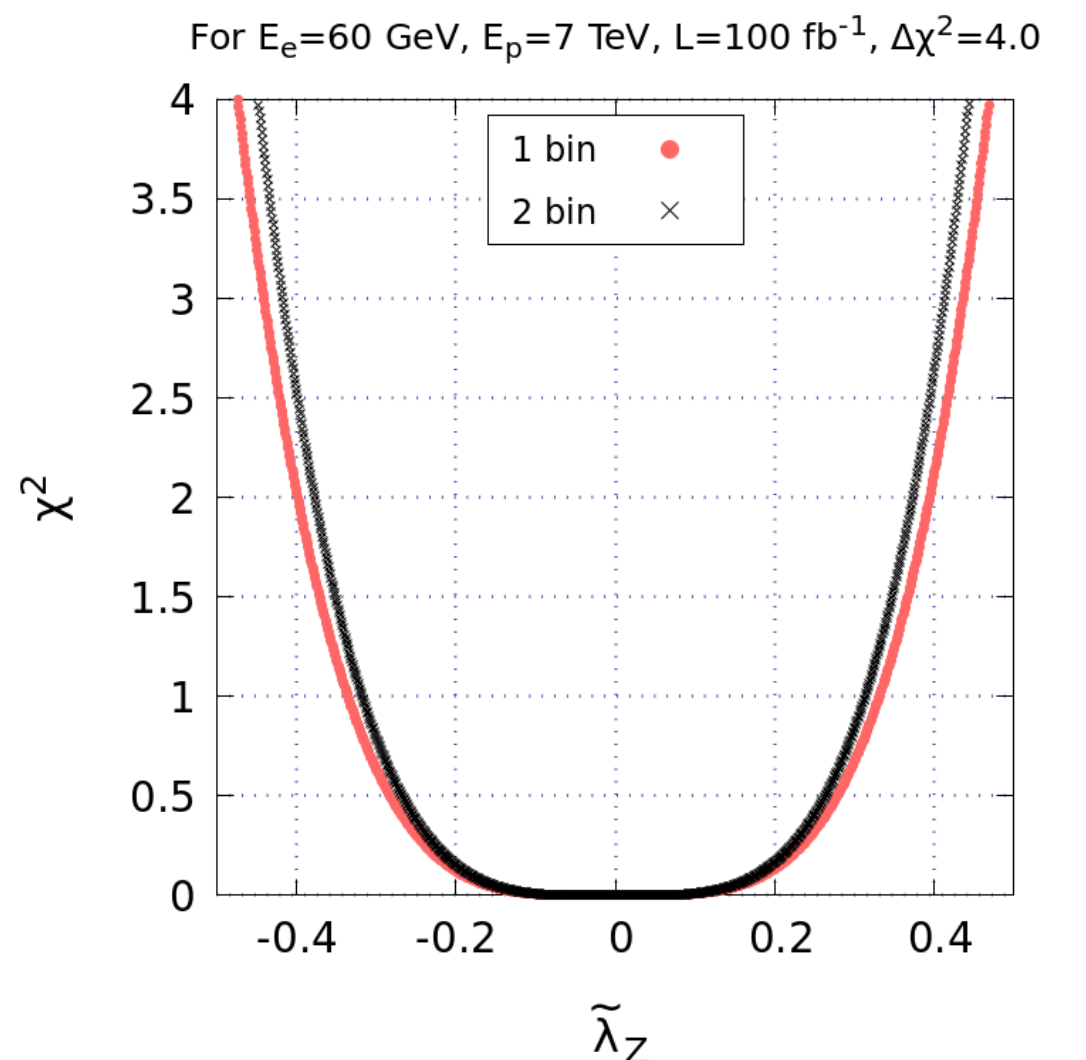
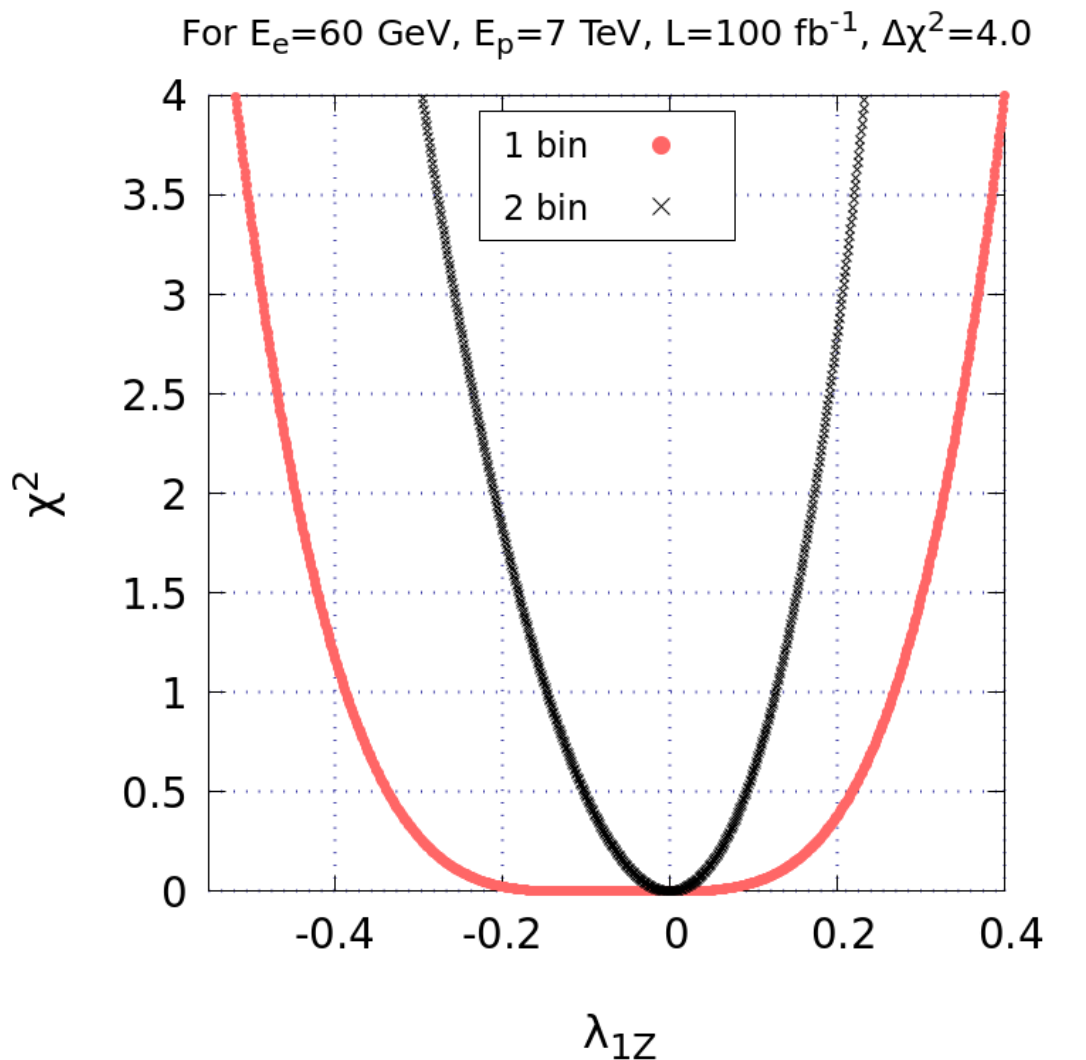
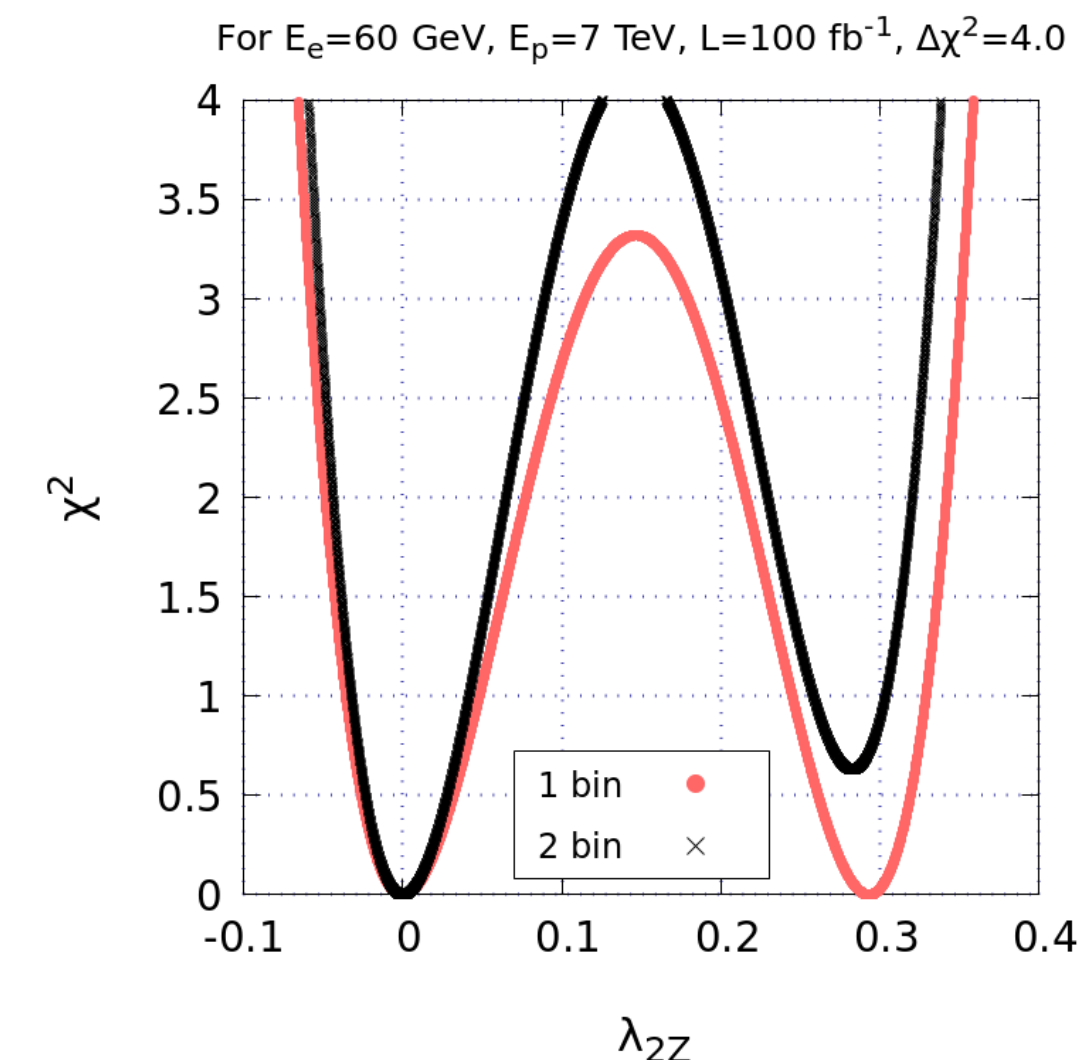
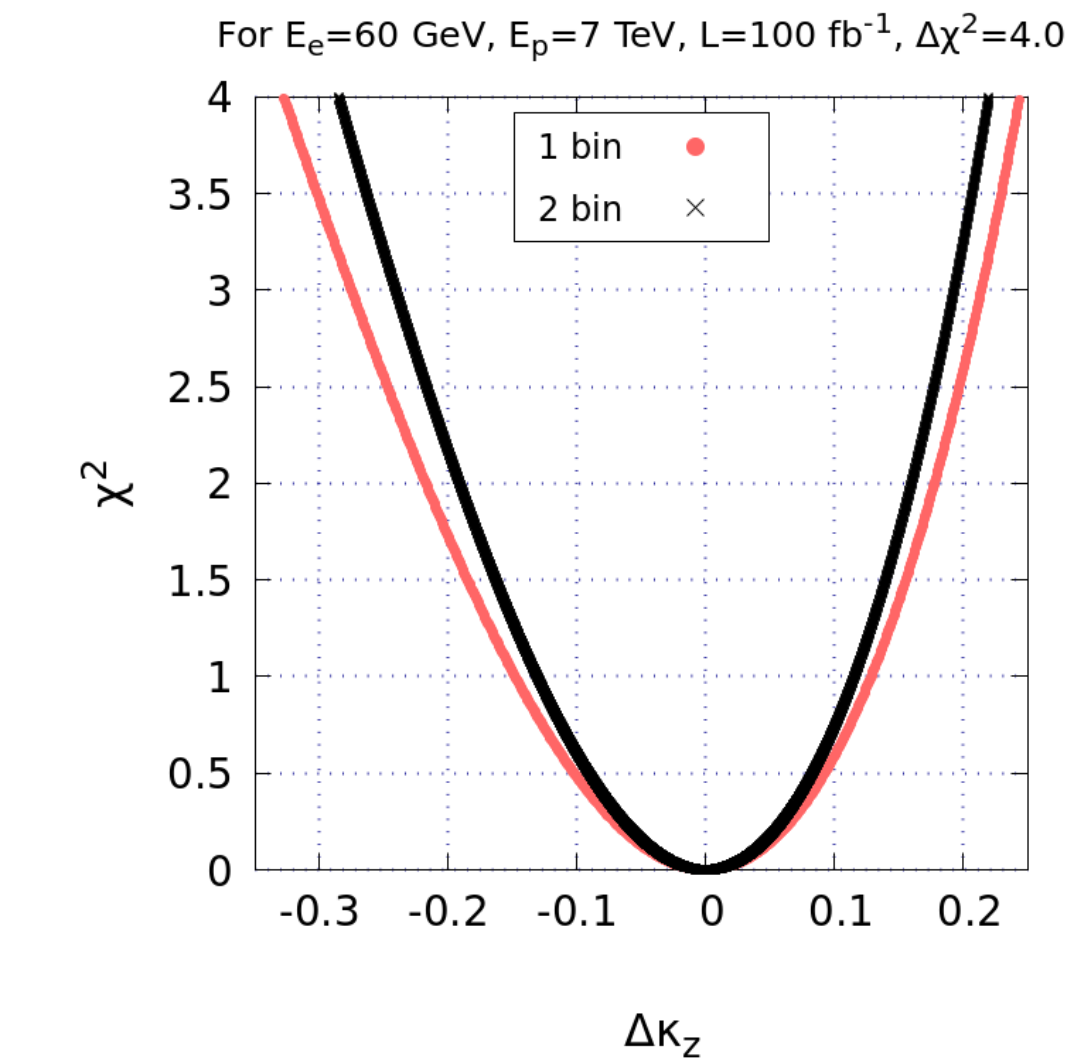
Results

$$\chi^2(c_i) = \sum_{j=1}^n \left(\frac{N_j^{\text{BSM}}(c_i) - N_j^{\text{SM}}}{\Delta N_j} \right)^2$$

↓
Suppress χ^2 due to huge background

- HZZ parameters less stringent as compared to HWW parameters
- All parameters lie within range $[-0.45, 0.45]$

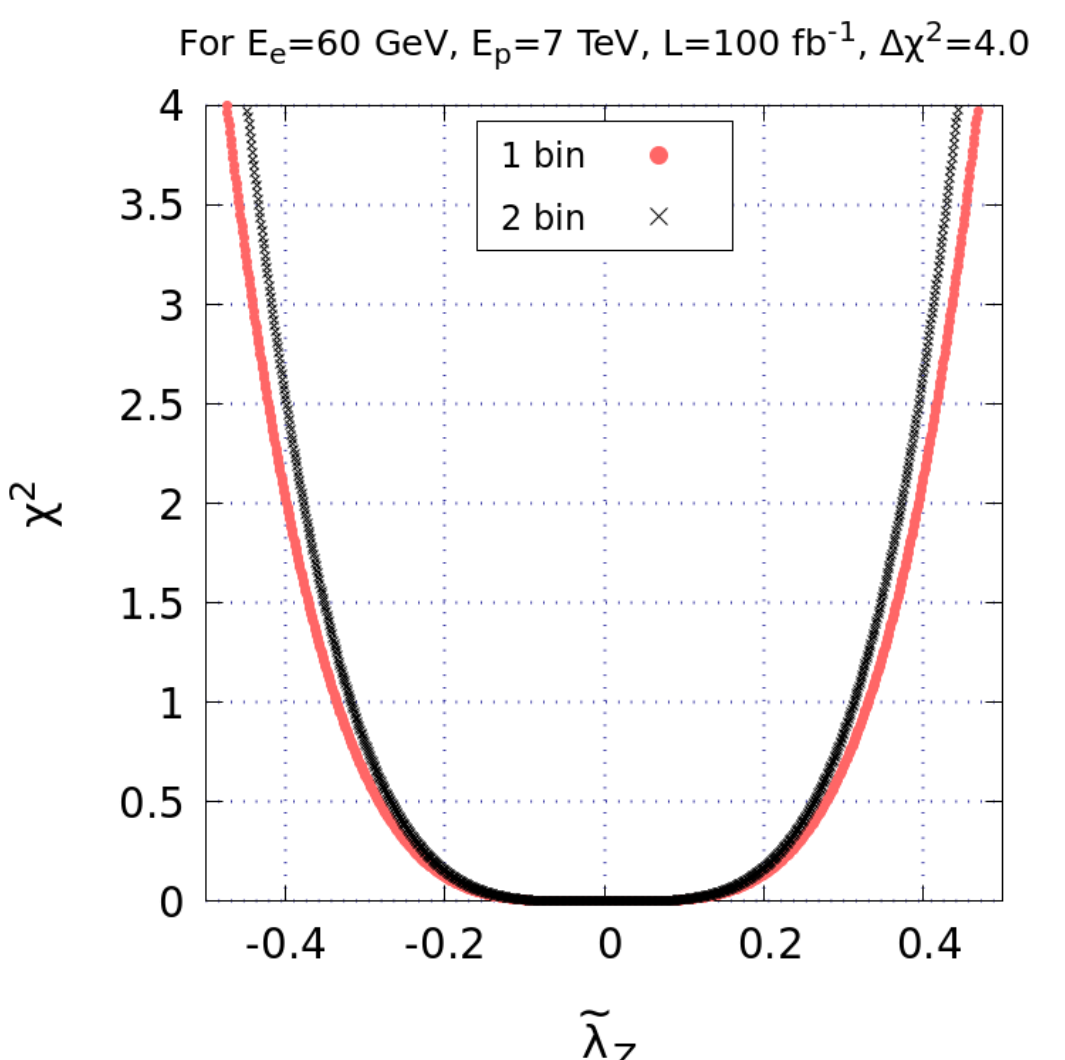
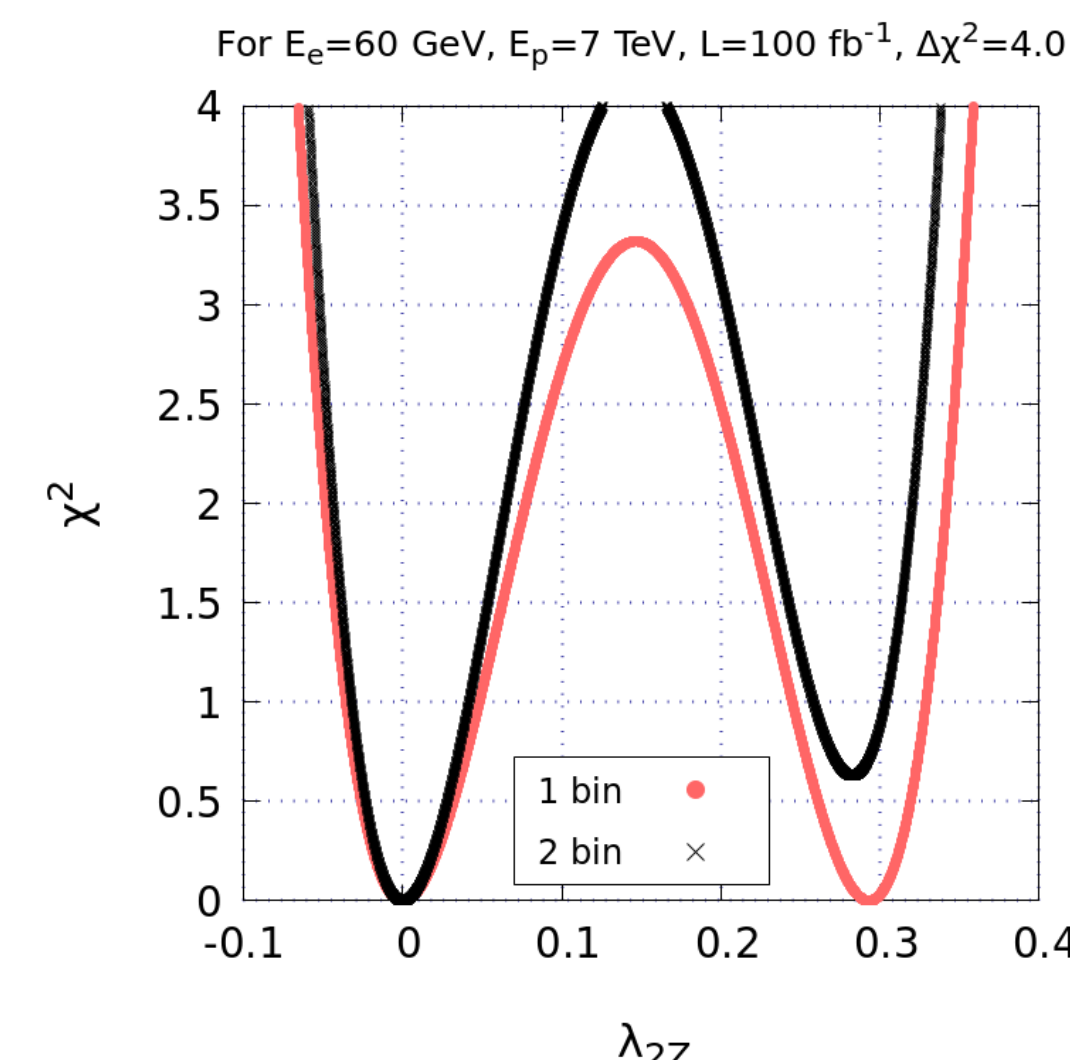
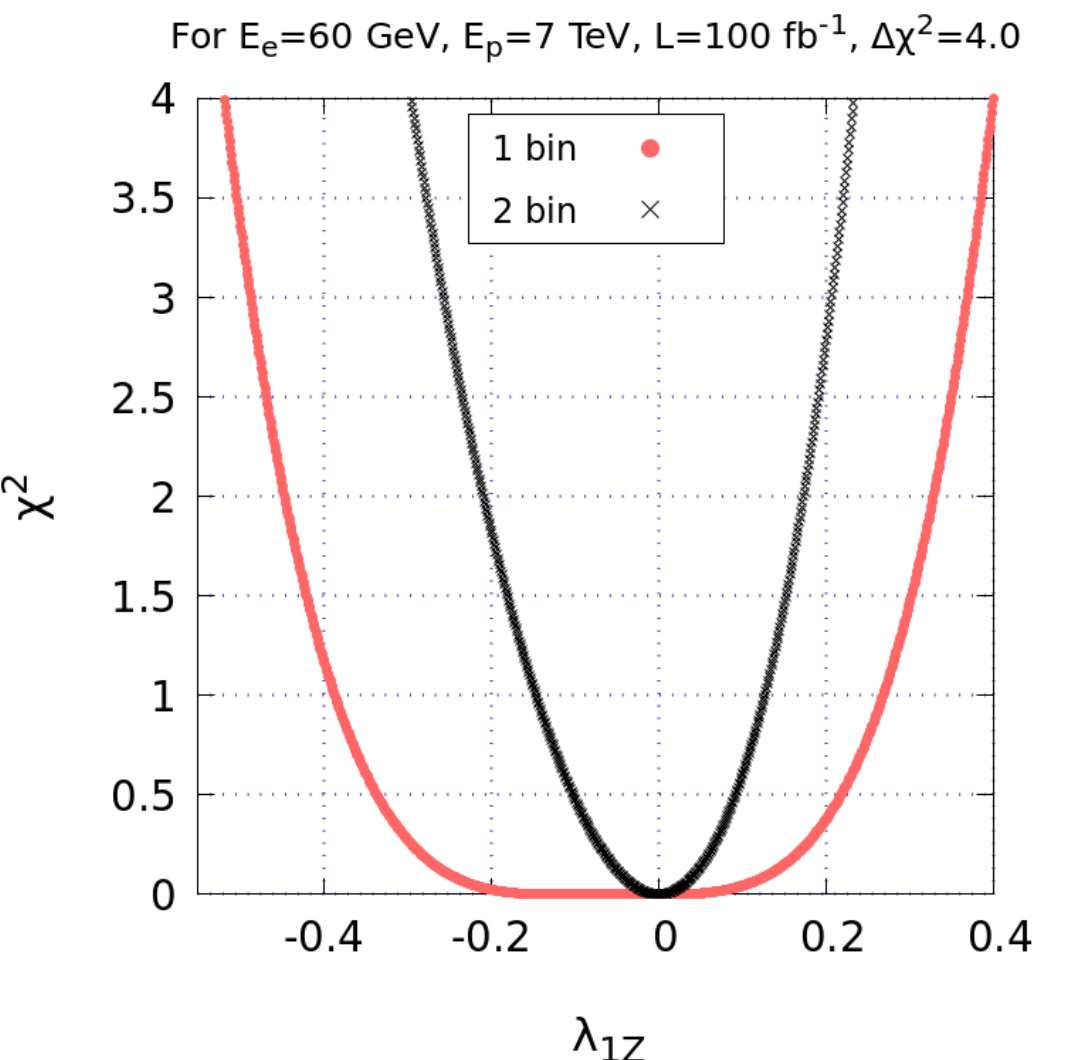
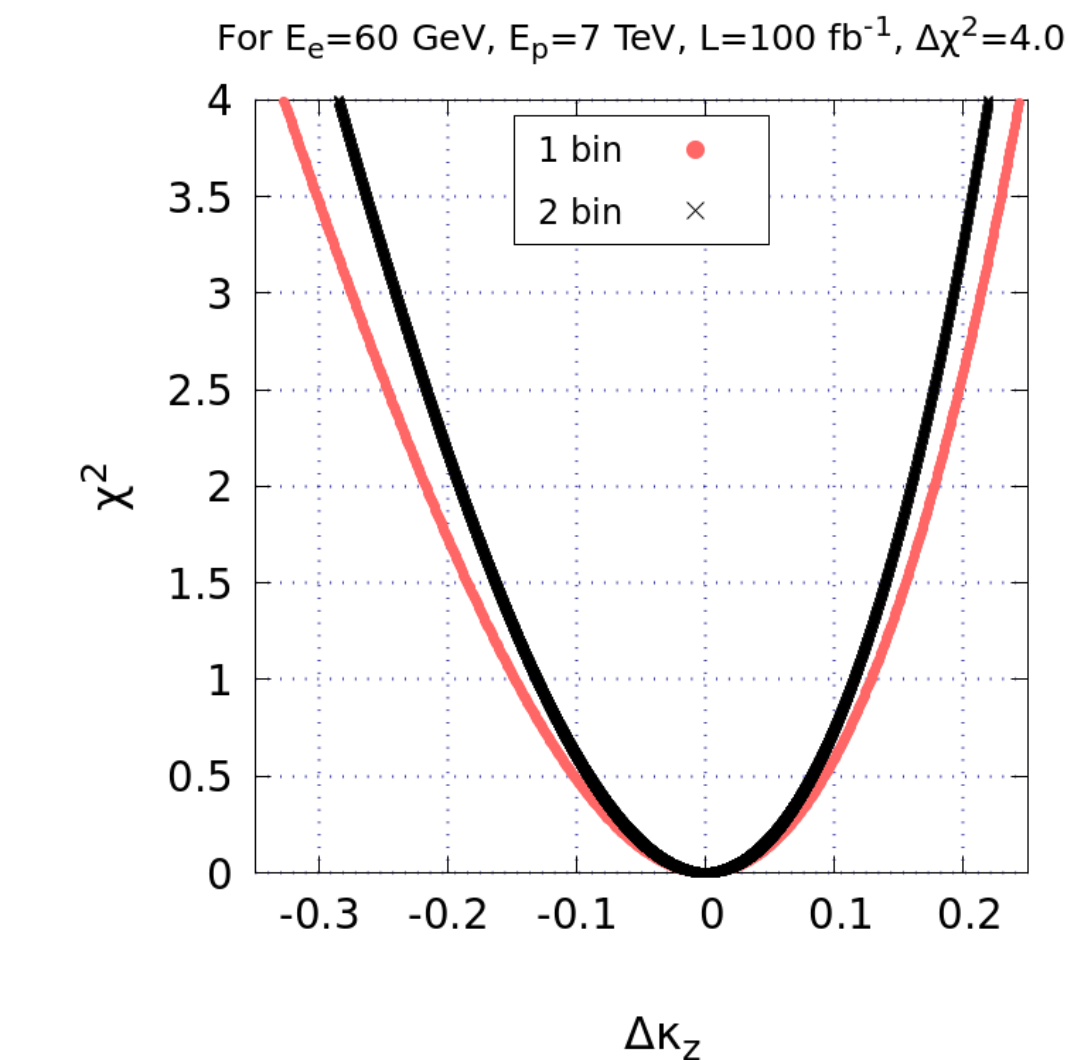
Constraints on HZZ parameters at $L = 100 \text{ fb}^{-1}$



at 95% C.L.

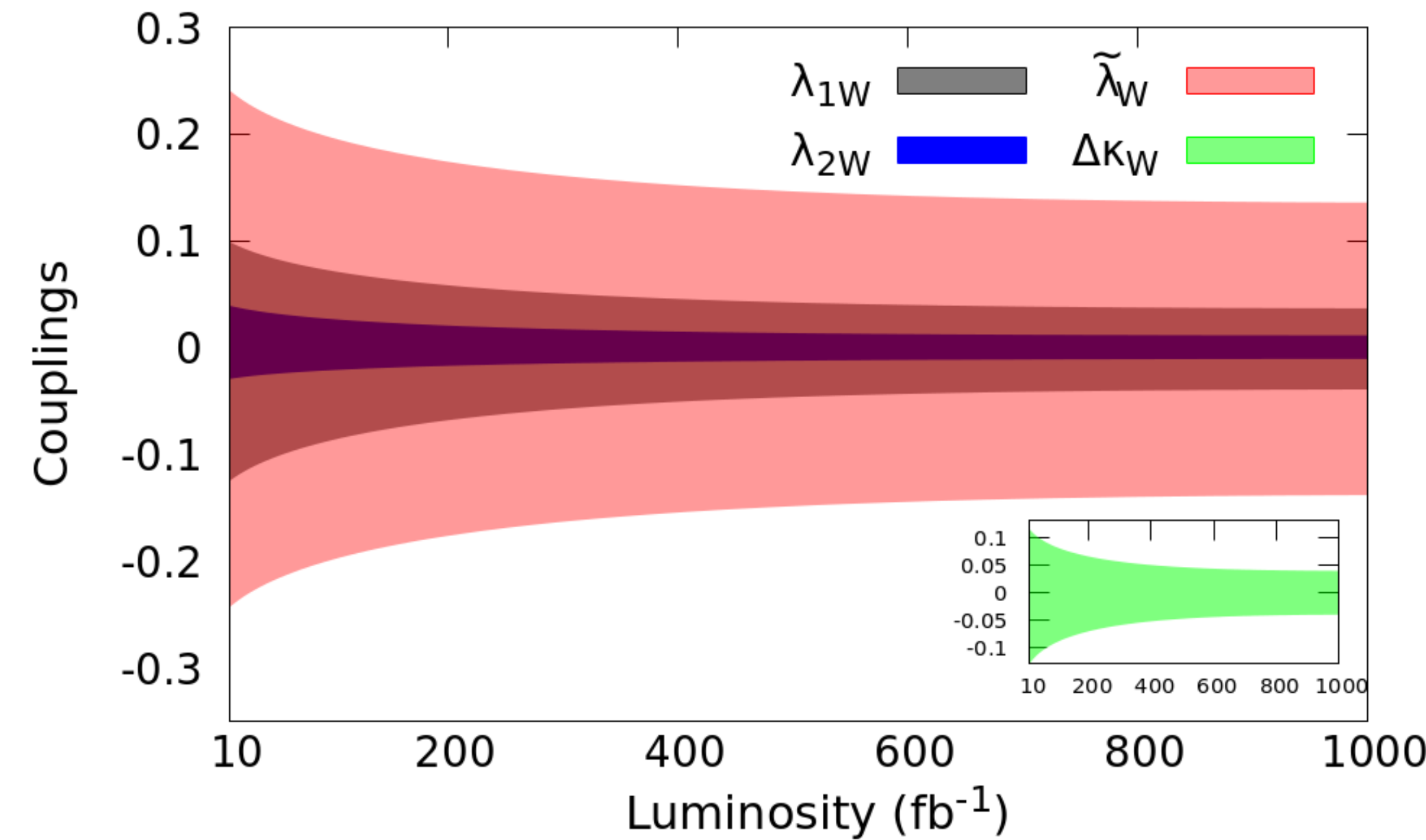
	Our limits at $L = 100 \text{ fb}^{-1}$	Run II data [a]	HL LHC [e]
$\kappa_Z \rightarrow$	[0.72, 1.22]	[0.75, 1.21]	3.0%
$\lambda_{1Z} \rightarrow$	[-0.35, 0.25]		HL LHC [g] [-0.01, 0.01]
$\lambda_{2Z} \rightarrow$	[-0.06, 0.13] \cup [0.17, 0.34]		HL LHC [g] [-0.007, 0.007]
$\tilde{\lambda}_Z \rightarrow$	[-0.45, 0.45]	Run II LHC [b] [-0.21, 0.15]	HL LHC [g] [-0.08, 0.08]

Constraints on HWW parameters at $L = 100 \text{ fb}^{-1}$



$$\Delta N \approx \sqrt{\sigma L} \quad (\text{for } \delta_{sys} = 0) \implies \chi^2 \propto L$$

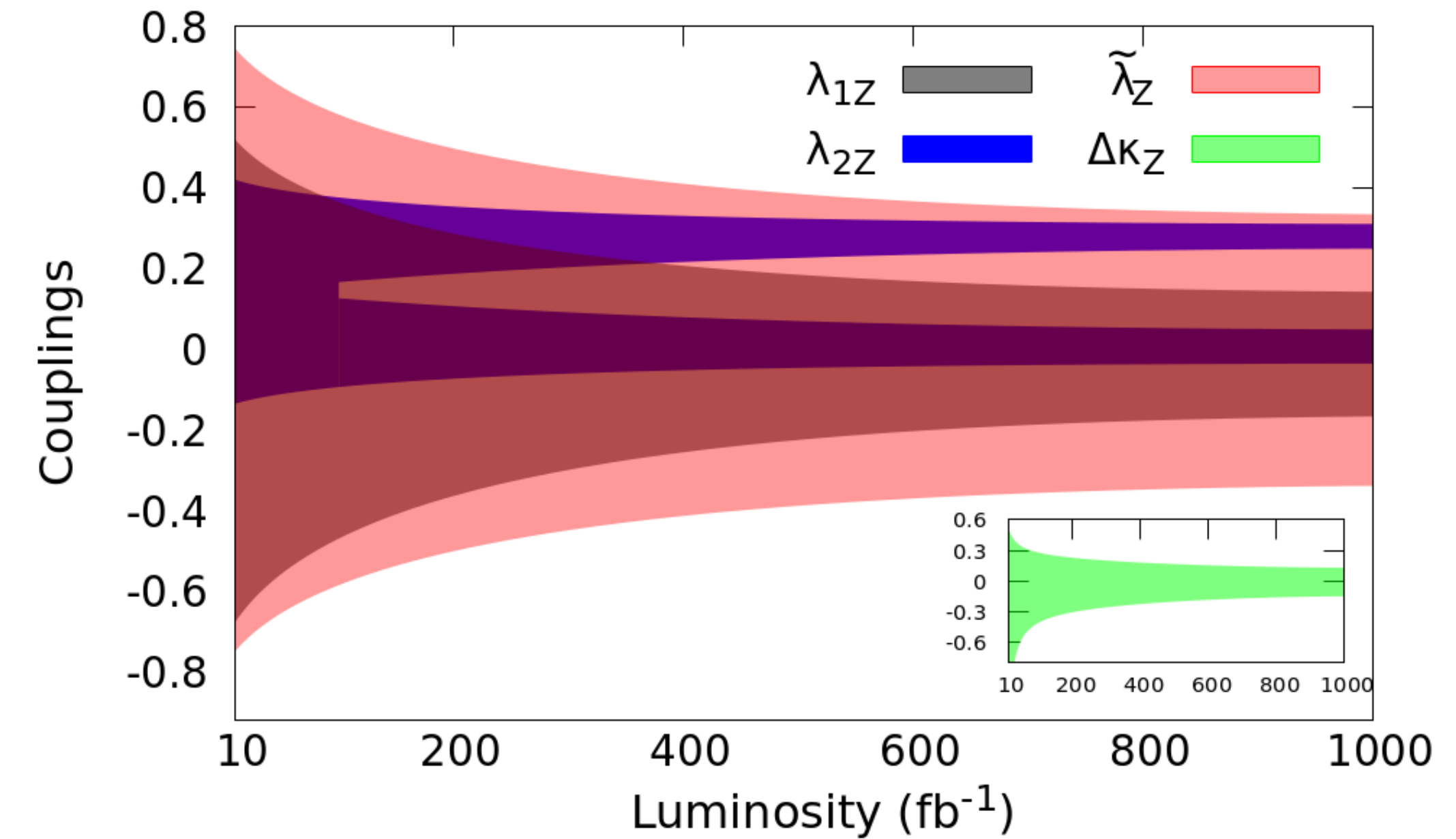
at 95% C.L.



Luminosity from 10 to 10^3 fb^{-1}

$\kappa_W, \lambda_{1W}, \lambda_{2W}, \tilde{\lambda}_W \rightarrow 67\%, 40\%, 78\%, 42\%$

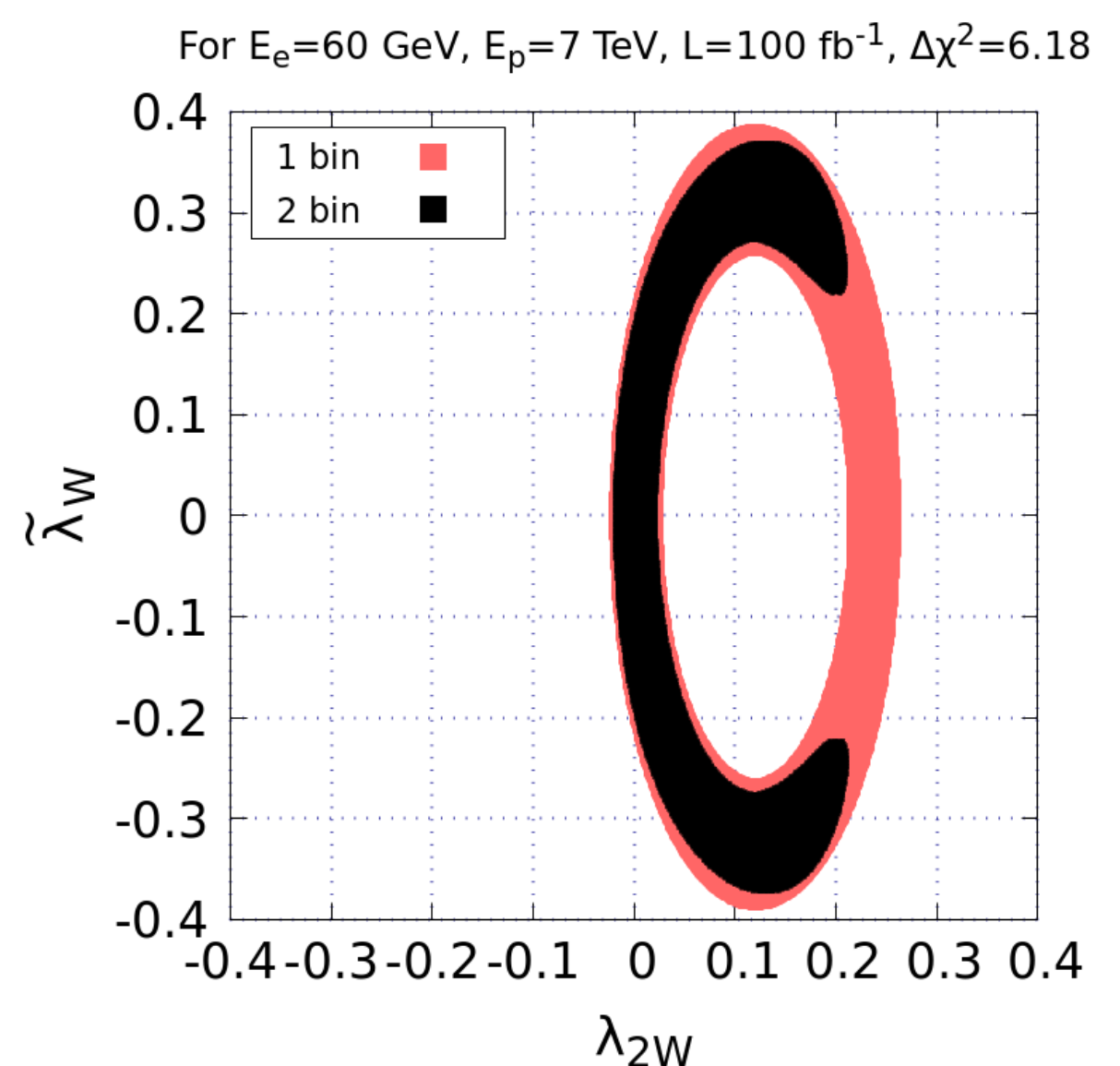
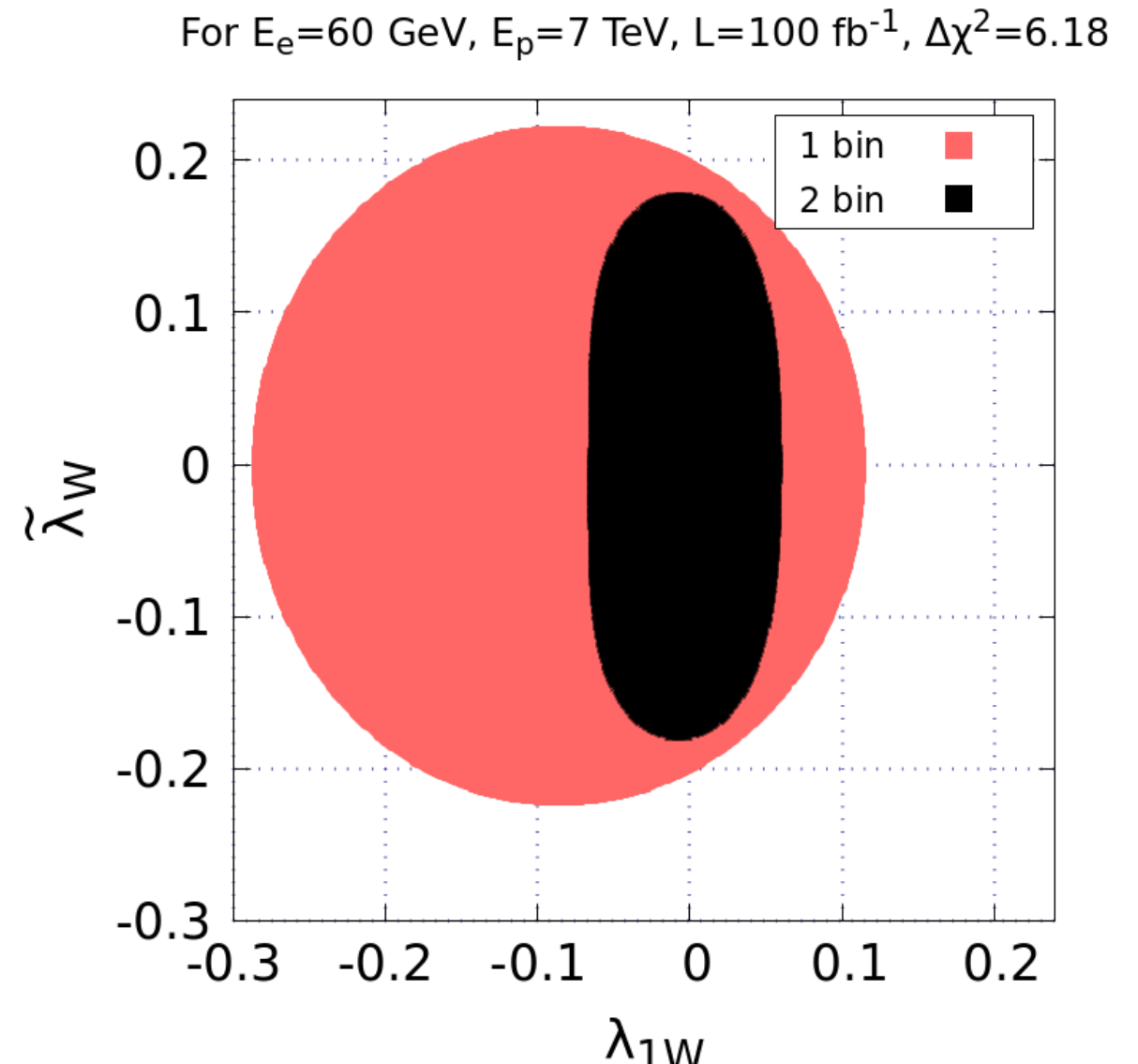
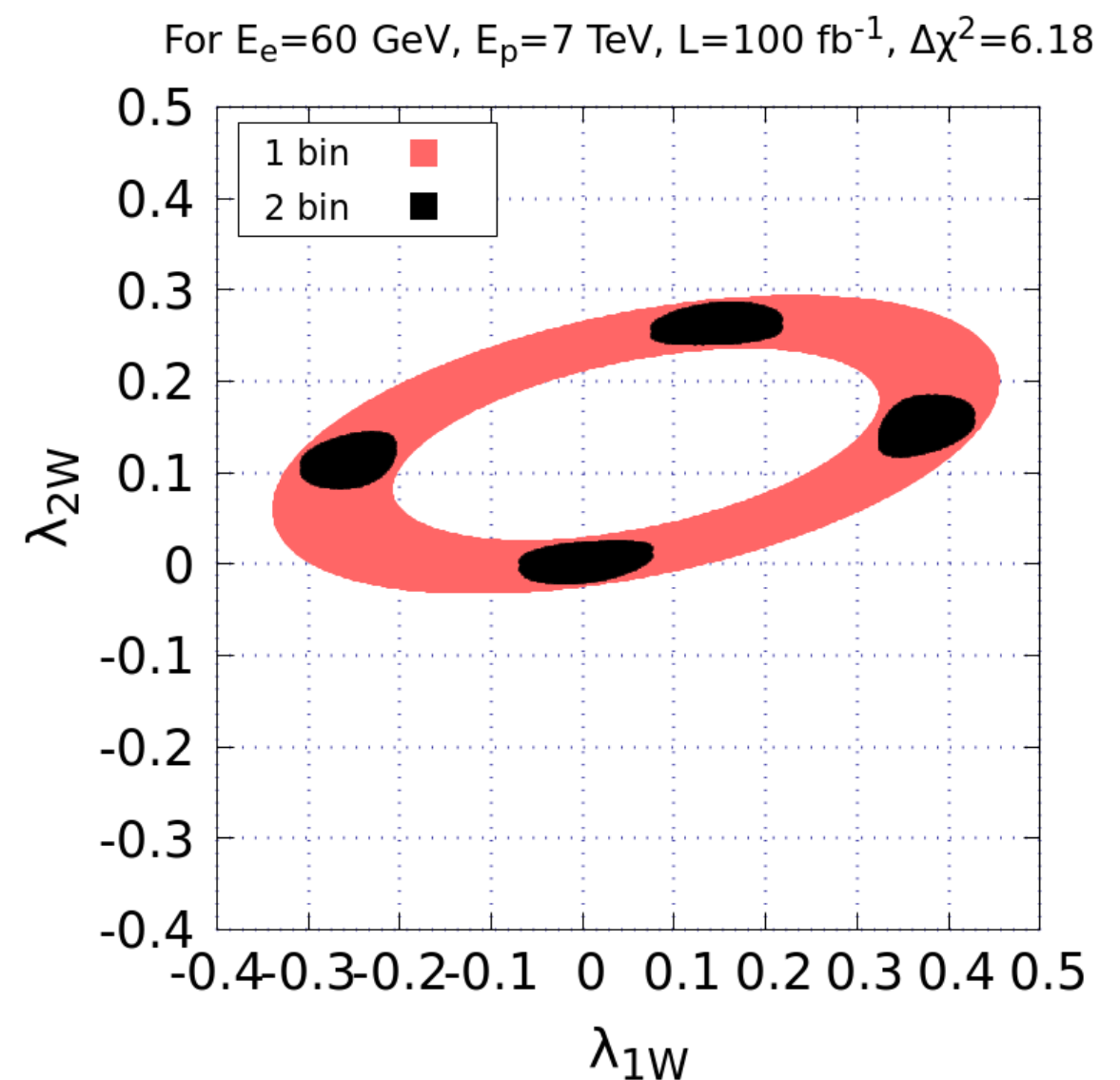
$\kappa_Z, \lambda_{1Z}, \lambda_{2Z}, \tilde{\lambda}_Z \rightarrow 91\%, 74\%, 73\%, 55\%$



two parameter analysis for HWW coupling

$$X^{\text{BSM}} = X^{\text{SM}} + \sum_i X_i c_i + \sum_{i,j} X_{ij} c_i c_j.$$

Correlation of two
BSM parameters

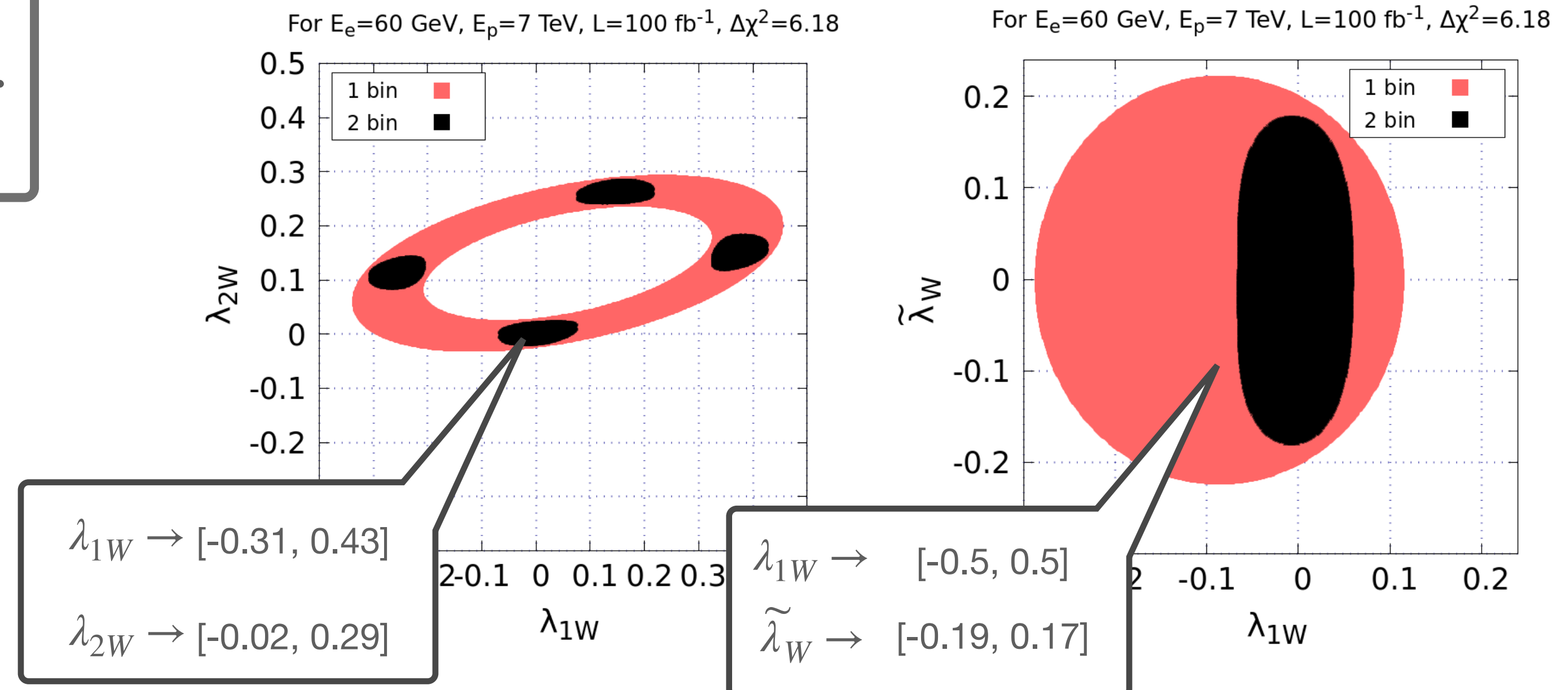


- Parameter space increases as going from one parameter to two parameter analysis
- $(\lambda_{1W}, \lambda_{2W})$ region is strongly correlated
- $(\lambda_{2W}, \tilde{\lambda}_W)$ region has least effect of 2 bin analysis

two parameter analysis for HWW coupling

$$X^{\text{BSM}} = X^{\text{SM}} + \sum_i X_i c_i + \sum_{i,j} X_{ij} c_i c_j.$$

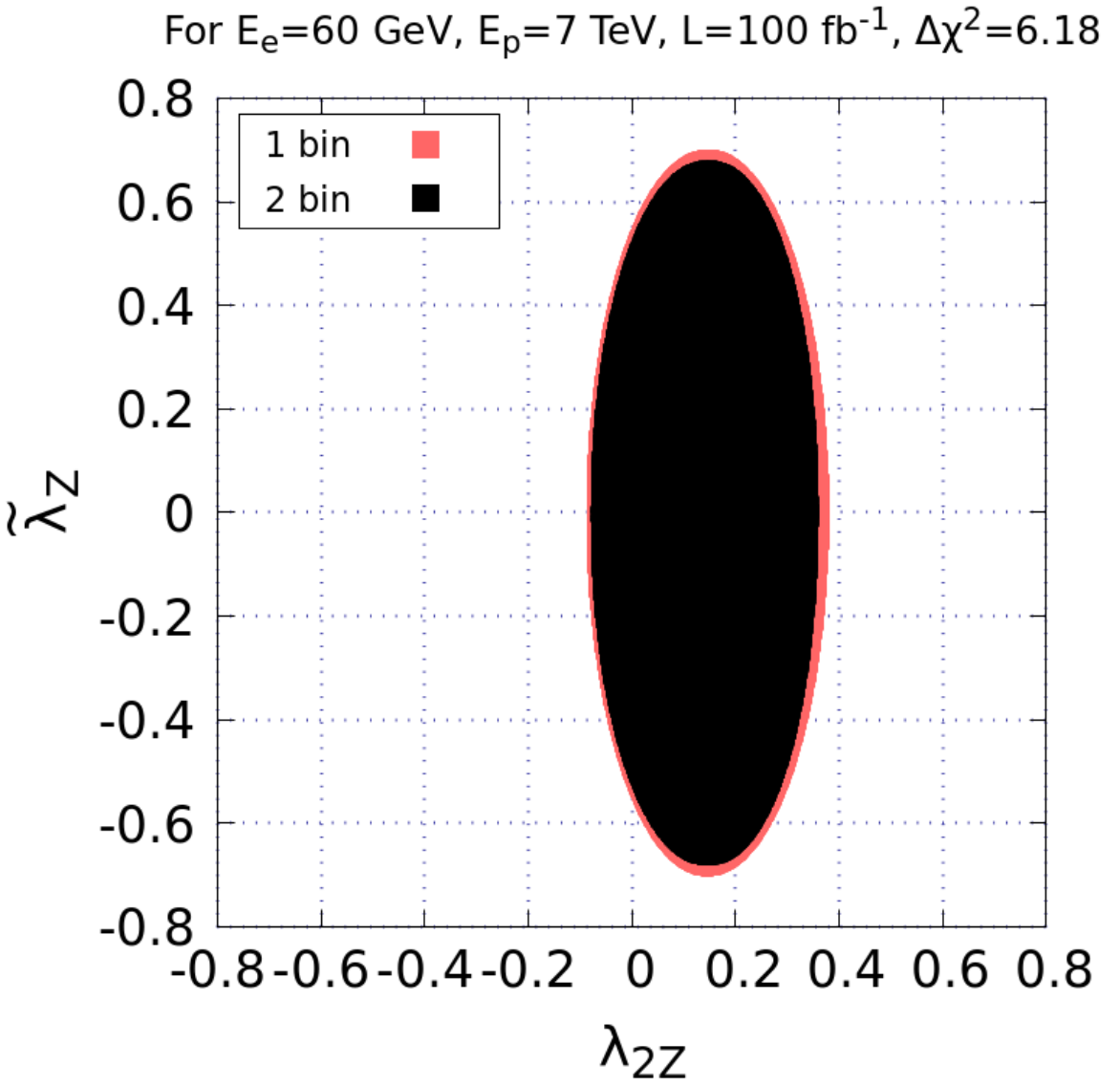
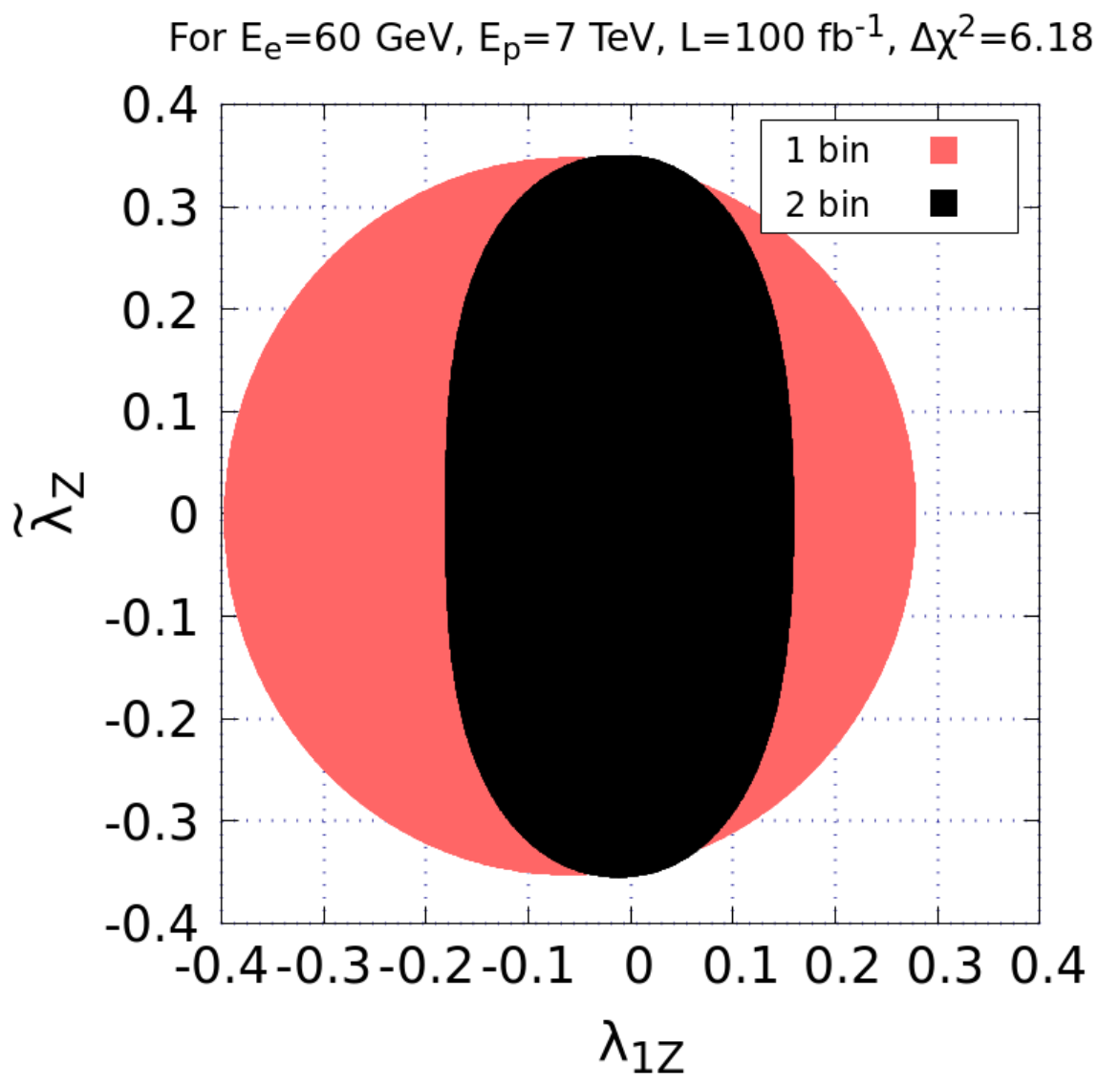
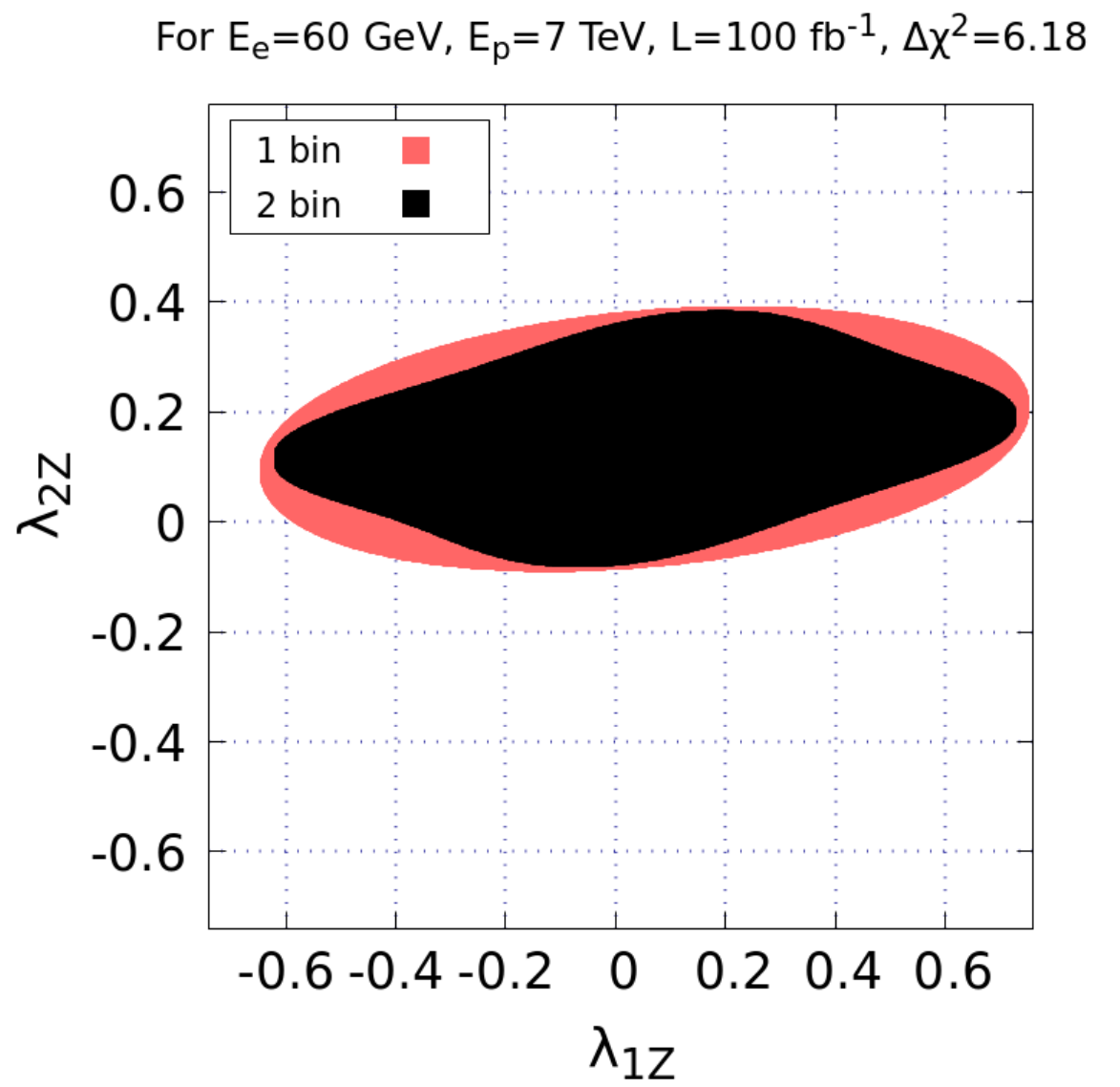
Correlation of two
BSM parameters



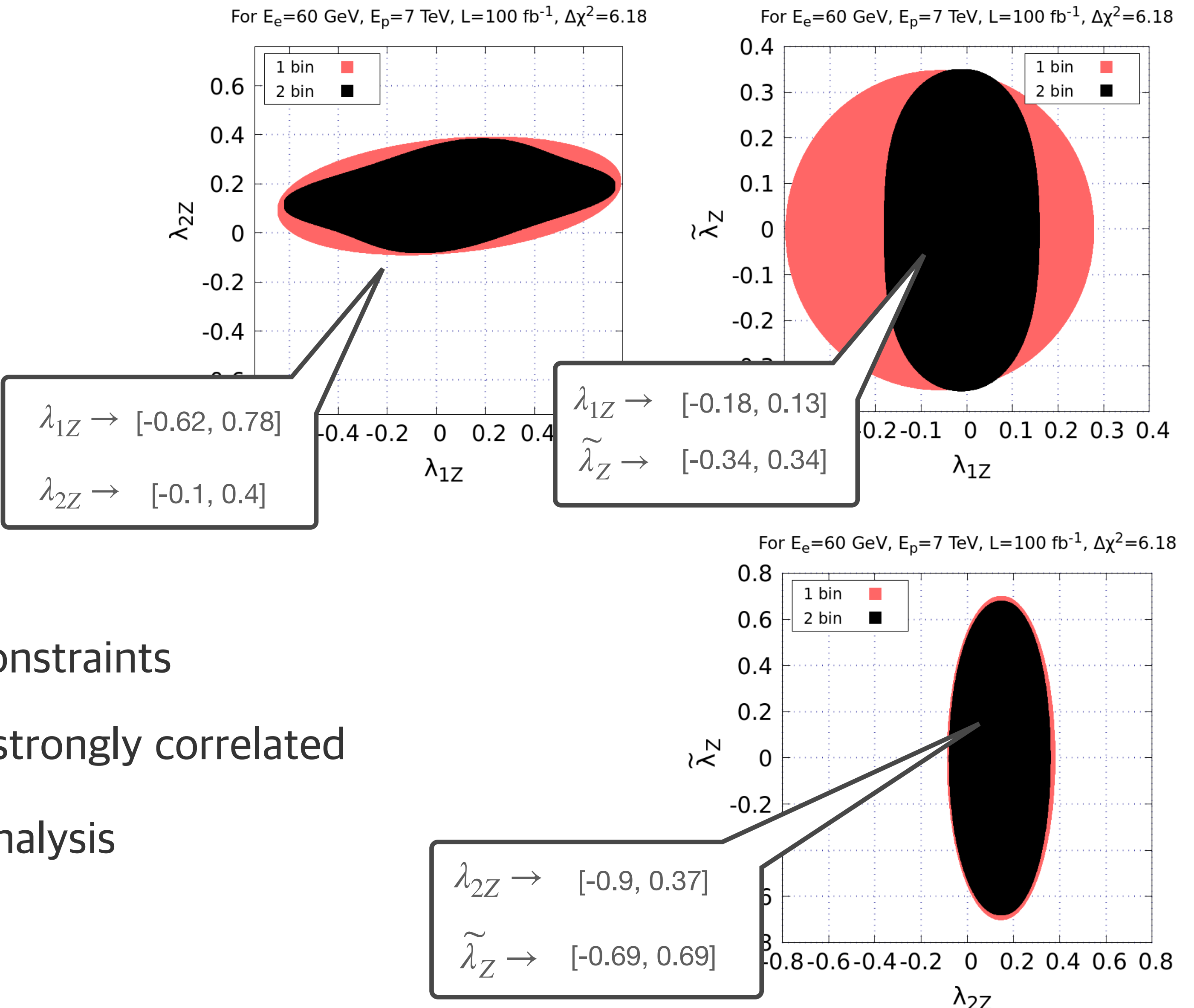
- Parameter space increases as going from one parameter to two parameter analysis
- $(\lambda_{1W}, \lambda_{2W})$ region is strongly correlated
- $(\lambda_{2W}, \tilde{\lambda}_W)$ region has least effect of 2 bin analysis

two parameter analysis for HZZ coupling

- 2 bin analysis is not efficient to improve constraints
- Like HWW case, $(\lambda_{1Z}, \lambda_{2Z})$ region is also strongly correlated
- $(\lambda_{2Z}, \tilde{\lambda}_Z)$ region has least effect of 2 bin analysis



two parameter analysis for HZZ coupling



- 2 bin analysis is not efficient to improve constraints
- Like HWW case, $(\lambda_{1Z}, \lambda_{2Z})$ region is also strongly correlated
- $(\lambda_{2Z}, \tilde{\lambda}_Z)$ region has least effect of 2 bin analysis

Conclusion

- $|\Delta\phi|$ distribution is sensitive to $HVV(V = W^\pm, Z)$ coupling.
- Using $|\Delta\phi|$ distribution, constraints are obtained keeping one parameter and two parameters non zero at a time.
- Constraints on BSM parameters are improved as going from 1 bin to 2 bin.
- Change in constraints as a function of luminosity is discussed.
- Constraints from two parameter analysis are loose as compared to one parameter analysis.

Back up

For BSM parameter c_i , χ^2 function is

$$\chi^2(c_i) = \sum_{j=1}^n \left(\frac{N_j^{\text{BSM}}(c_i) - N_j^{\text{SM}}}{\Delta N_j} \right)^2$$

N_j^{SM} and $N_j^{\text{BSM}} \rightarrow$ SM and BSM events in j^{th} bin

uncertainty (Statistical + systematic)

$$\Delta N_j = \sqrt{N_j^{\text{SM+Bkg}} \left(1 + \delta_{\text{sys}}^2 N_j^{\text{SM+Bkg}} \right)}$$



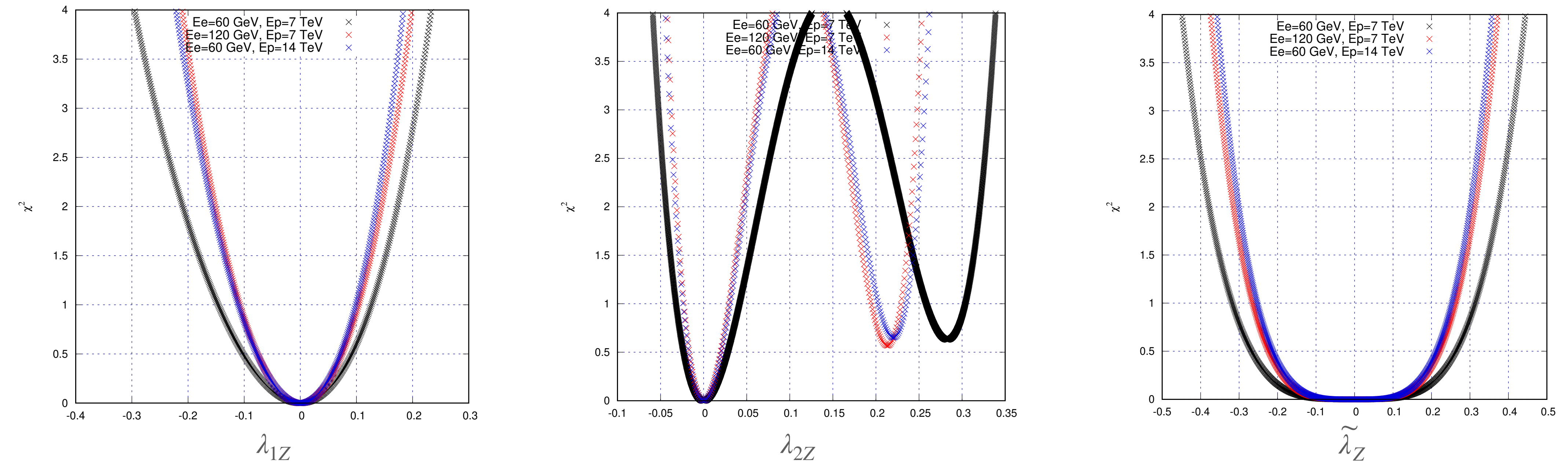
↓
5%

$$\sqrt{N_j^{\text{SM+Bkg}}} = \sqrt{\sigma_j^{\text{SM+Bkg}} L}$$

Back up

- $e^- p \rightarrow \nu_e b\bar{b} jj$ has 2 events after cuts
- $e^- p \rightarrow e^- jjj$ has 15 events and S/B changes 0.41 to 0.38
 - PDF: NN23LO1
Uncertainty: 2.5%
 - Renormalisation factorisation scale choice: -1 in MadGraph which is related to the transverse energy of the final state particles
Uncertainty: 5%

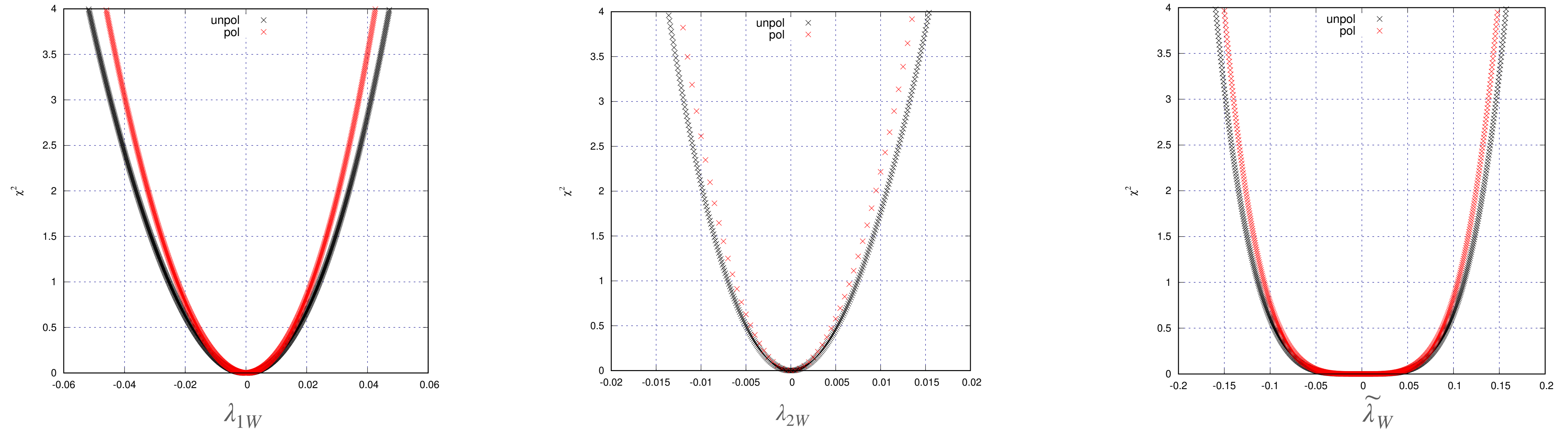
Back up



Constraints on HZZ parameters with respect to energy

- Constraints are improved by increasing energy

Back up



Constraints on HWW parameters for -80% e-beam polarisation

- For -80% e-beam polarization S/B = 11.0 (CC) and 0.3 (NC)
No significant improvement in NC but constraints improved by 7-10% in CC case.